Overview of Arctic Cloud and Radiation Characteristics

JUDITH A. CURRY,* WILLIAM B. ROSSOW,+ DAVID RANDALL,@ AND JULIE L. SCHRAMM*

*University of Colorado, Boulder, Colorado
+NASA/Goddard Institute for Space Studies, New York, New York
@Colorado State University, Fort Collins, Colorado

(Manuscript received 18 January 1995, in final form 15 February 1996)

ABSTRACT

To provide a background for ARM's activities at the North Slope of Alaska/Adjacent Arctic Ocean sites, an overview is given of our current state of knowledge of Arctic cloud and radiation properties and processes. The authors describe the Arctic temperature and humidity characteristics, cloud properties and processes, radiative characteristics of the atmosphere and surface, direct and indirect radiative effects of aerosols, and the modeling and satellite remote sensing of cloud and radiative characteristics. An assessment is given of the current performance of satellite remote sensing and climate modeling in the Arctic as related to cloud and radiation issues. Radiation–climate feedback processes are discussed, and estimates are made of the sign and magnitude of the individual feedback components. Future plans to address these issues are described.

1. Introduction

The importance of cloud–radiative interactions to global climate has been highlighted by many investigators (e.g., Wetherald and Manabe 1988; Mitchell and Ingram 1992) and has provided the motivation for numerous scientific programs, including the Atmospheric Radiation Measurement (ARM) program. An understanding of cloud–radiative interactions in the Arctic has remained particularly enigmatic, and ARM has thus proposed the North Slope of Alaska and Adjacent Arctic Ocean (NSA/AAO) as a primary measurement site. Until recent climate modeling results highlighted the Arctic as a region of particular importance and vulnerability to global climate change (e.g., IPCC 1990), there has been little motivation to focus on the physical processes occurring in the Arctic climate system, which are in many ways unique compared with other regions of the globe. Arctic sea ice drastically affects air–sea energy exchanges by greatly increasing the surface albedo and by insulating the very cold winter atmosphere from the relatively warm ocean water below the ice. In addition, the flow of Arctic ocean water and sea ice into the North Atlantic is aimed directly at the deep-water formation zone, which is a lynch pin of the global ocean thermohaline circulation (e.g., Broecker et al. 1988). The importance of high-latitude cloud processes to global climate are highlighted by issues related to: the impact of cloud–radiative processes on the stability of Arctic Ocean pack ice (e.g., Curry et al. 1993); the impact of high-latitude precipitation on the global ocean thermohaline circulation (e.g., Broecker et al. 1989); and the potential thawing of the permafrost that could release tremendous stores of carbon to the atmosphere (e.g., Cappellaz et al. 1993).

Of central importance to our understanding of the Arctic climate system is the ability to understand and model cloud and radiation processes and their interrelationship with atmospheric dynamics and the underlying boundary. The effect of clouds on radiation is very complex over the Arctic particularly due to the presence of the highly reflecting snow and ice, the absence of solar radiation for a large portion of the year, low temperatures and water vapor amounts, and the presence of temperature inversions. An understanding and correct simulation of the cloud–radiative feedback mechanism requires understanding of changes in: cloud fraction and vertical distribution as the vertical temperature and humidity profiles change and changes in cloud water content, phase and particle size as atmospheric temperature and composition changes. In the Arctic, the cloud–radiation feedback is inextricably linked with the snow/ice albedo feedback. It has been hypothesized that changes in surface albedo associated with changes in snow and ice cover as a result of temperature changes provides a significant positive feedback on climate change.

Four unusual cloudy boundary-layer types have been identified over the Arctic Ocean: (i) summertime boundary layer with multiple layers of cloud; (ii) mixed-phase boundary-layer clouds that occur in the transition seasons; (iii) low-level ice crystal clouds and "clear sky" ice crystal precipitation in stable winter-

Corresponding author address: Dr. Judith A. Curry, Department of Aerospace Engineering Sciences, Engineering Center, University of Colorado, Campus Box 429, Boulder, CO 80309-0429.

time boundary layers; and (iv) wintertime ice crystal plumes emanating from leads, or cracks, in the sea ice. These unusual boundary-layer types provide a substantial challenge to atmospheric models and also to observational strategies currently used for the cloudy boundary layer.

Climate model parameterizations of clouds, radiation, and other processes involved in the evolution of cloud systems (e.g., precipitation, boundary layer, and surface processes) have been developed for environments with vastly different thermodynamic characteristics than are found in the Arctic. Numerical weather prediction and mesoscale modeling studies have not focused on the Arctic atmosphere, and little diagnostic work or specific parameterization development for that region has been undertaken. As a result, even our basic understanding of the physical process occurring in Arctic weather systems is deficient (e.g., Bromwich et al. 1994).

Arctic clouds also present unique challenges for satellite remote sensing, and the largest errors in ISCCP (International Satellite Cloud Climatology) cloud properties and ERBE (Earth Radiation Budget Experiment) cloud–radiative forcing occur in the polar regions (e.g., Rossow et al. 1993; Ramanathan et al. 1989). The determination of polar cloud characteristics using current satellite observations encounters significant obstacles. The Arctic clouds are predominantly optically thin and low lying. Because of the state of the underlying snow/ice surface, there is little visible, thermal, or microwave contrast between the clouds and the underlying surface, and standard thresholding techniques are inadequate. Moreover, Arctic atmospheric conditions create unusual amounts of near-surface hazes and fogs that exhibit little signature in satellite observations (e.g., Rossow and Garder 1993) and may even exhibit reversed contrast in both visible and infrared measurements (e.g., Raschke et al. 1992). Improvements to satellite cloud retrievals are severely hampered by the lack of validation data in the Arctic.

To provide a background for ARM's activities at the North Slope of Alaska/Adjacent Arctic Ocean (NSA/AAO) sites, an overview is given here of our current state of knowledge of Arctic cloud and radiation properties and processes: temperature and humidity characteristics; cloud processes and characteristics; radiative characteristics of clear sky, clouds, and surface; direct and indirect radiative effects of aerosols; and the modeling and satellite remote sensing of cloud and radiative characteristics. No attempt has been made to be encyclopedic in this discussion or to include all related papers; rather, the emphasis here is on describing the key works that have influenced our understanding of the relevant processes and citing papers that present data and observations in a useful way. Polar stratospheric clouds are not considered here since optical depths are less than 0.1 (e.g., Kent et al. 1986) and thus do not substantially perturb the atmospheric radiation.

2. Temperature and humidity

Surface air temperatures from 1931 through 1966 at Barrow, Alaska, are summarized by Maykut and Church (1973) to have a monthly minimum in February of −28°C and a maximum in July of 3.9°C, with the lowest and highest recorded temperatures being −49°C and 25°C. A summary of the annual cycle of Arctic Ocean sea ice surface temperature is presented by Lindsay and Rothrock (1994a). Key and Haefliger (1992) describe a technique for retrieving Arctic Ocean surface temperature from the two infrared channels from AVHRR. Based on these studies, the monthly mean surface temperatures in the central Arctic range from −35° to −40°C in March to −1.5°C in June with a rapid warming beginning in April and a rapid cooling beginning in September. Key et al. (1994) compared surface-based measurements of surface air temperature, radiometrically determined "skin" surface temperature, and a snow temperature measured just below the surface during May and found that the surface skin temperature is approximately 1°C warmer than the surface air temperature.

The dominant feature of the atmospheric temperature and humidity fields in the Arctic is the presence of temperature and humidity inversions, particularly during the coldest half of the year. Temperature increases with height in the lower troposphere may exceed 30°C on individual days during winter. Extremely stable conditions may persist for many weeks, essentially decoupling the surface from conditions in the lower troposphere. The definition of a "temperature inversion" varies among authors. We adopt the convention used by Kahl (1990) and Serreze et al. (1992) to define inversions as layers in which temperature increases with altitude but include thin embedded layers with a decrease of temperature with height provided they are not more than 100 m in depth.

The first detailed studies of the vertical temperature and humidity profiles over the Arctic Ocean were made by Sverdrup (1933) during the *Maud* expedition using kite and captive balloon ascents, indicating ubiquitous lower-troposphere surface temperature and humidity inversions. Using data from an ice island, Belmont (1957) noted the complexity of the inversion, with multiple inversion layers frequently observed. Vowinckel and Orvig (1970) made the first attempt to describe regional variations of the temperature inversion. The databases describing Arctic in situ sounding data are summarized by Kahl et al. (1992). Detailed statistics on temperature inversion characteristics (depth, frequency, temperature gradient) have been provided by Kahl (1990) along the Alaskan Coast, Kahl et al. (1992) in the Canadian Arctic, Bradley et al. (1992) in the North American Arctic, and Serreze et al. (1992)

in the Eurasian Arctic and Arctic Ocean. Of particular interest to the ARM NSA site at Barrow, Kahl (1990) found that surface-based inversions occur nearly half of the time, median inversion depths range from 250 m in autumn to 850 m in late winter, and the median temperature difference across the inversion ranges from 11°C in late winter to 2°C during early autumn. The deepest inversions are found over the interior of the pack ice during winter, with an average inversion depth of 1200 m, and inversions are found constantly from December through April. The minimum frequency of inversions in the central Arctic is 85% during August, when the median inversion depth is 400 m. The median temperature differences across the inversions are 12.6°C during winter and 2.8°C during August. Skony et al. (1994) point out that there are significant differences between radiosonde and dropsonde temperature profiles over the Arctic Ocean arising from contrasting temperature lag errors accompanying ascending and descending sensors. Using an acoustic sounder to study the Fairbanks temperature inversions, Holmgren et al. (1975) pointed out the complexity of structure in situations with well-developed inversions, with as many as 10–20 separate backscatter bands within the height interval from the surface up to 500 m.

Wexler (1936) was the first to address the physical controls behind the formation of Arctic temperature inversions. Wexler approached this problem by considering the radiative equilibrium between the snow surface and the overlying atmosphere. Snow radiates nearly as a blackbody in the infrared, much of the emitted energy escaping to space through the water vapor window. As the snow surface cools, the overlying atmosphere begins to cool by losing energy to the cold snow surface. The cooling atmosphere returns energy to the snow surface less rapidly than the surface loses heat, allowing the snow surface to continue cooling. In making his calculations, Wexler assumed that the vertical structure of the cooled air consisted of a temperature inversion in a thin layer at the ground surmounted by an isothermal layer. After 26 days of cooling, the modeled cool air is 4 km deep, the temperature of the isothermal layer having dropped to −35°C. Wexler concluded that the maximum rate of cooling occurs under calm, cloudless conditions.

In addition to radiative cooling, the physical processes that contribute to the evolution of the temperature inversion include warm air advection, subsidence, cloud processes, surface melt, and topography (Vowinkel and Orvig 1970; Maykut and Church 1973; Busch et al. 1982; Curry 1983; Kahl 1990). Curry (1983) expanded the theory of the formation of temperature inversions using a one-dimensional model that included radiative transfer, cloud microphysical processes, turbulent mixing, and subsidence. The rate of cooling and the vertical structure of the temperature inversion was shown to be very sensitive to the amount of condensed water in the atmosphere. Condensate is produced in the model primarily by radiative cooling and is depleted from the atmosphere primarily by gravitational settling (unlike Wexler's calculation, the modeled condensate does not immediately fall out). Radiative cooling from the condensate dominates the atmospheric radiative cooling, extending the cooling over an increasingly deepening layer as the depth of the condensate grows. Gravitational settling of the ice crystals significantly increases the amount of atmospheric radiative cooling by decreasing the opacity of the condensate. Thus, clouds are responsible for enhanced cooling of the atmosphere and retarded cooling of the surface. Subsidence modifies the formation of the temperature inversion by reducing the supply of moisture for condensation, thus influencing the radiative cooling. When compared with Wexler's calculation, Curry's cloudy model produced the same amount of cooling in 14 days (compared with 26 days for Wexler's model), but the surface remained at higher temperatures throughout. The gravitational settling of the ice crystals that form in the cooling air was shown to be responsible for the formation of a humidity inversion.

Atmospheric water vapor characteristics at 70°N are described by Serreze et al. (1995a), determining the zonal and monthly mean vertically integrated precipitable water to range from 2.9 mm in February and March to 16.2 mm in July. Over the Arctic Ocean, Serreze et al. (1995b) found that the average precipitable water for 80°–90°N is 1.8 mm during winter, with a July maximum of 12.5 mm. Curry et al. (1995b) examined the relationship between monthly values of surface temperature T_s and precipitable water W. It was shown that W increases with T_s, although this increase does not follow the general shape of the Clausius–Clapeyron curve, as was found by Stephens (1990) for low-latitude marine regions. A steep increase of precipitable water between 0° and 5°C arises during summertime when the sea ice is constrained to be at the melting point, while precipitable water shows large variations associated with the large-scale advection of moisture. The slow increase of precipitable water with surface temperature for temperatures lower than −15°C arises from the control of precipitable water by ice saturation at the lower temperatures, consistent with the physical processes described by Curry (1983) for the formation of temperature and humidity inversions.

Because of the paucity of conventional observations of temperature and humidity over the Arctic Ocean, there is increasing interest in using satellite-borne sensors. The *TIROS-N* Operational Vertical Sounder (TOVS) allows temperature and humidity profiles to be determined using measured infrared and microwave radiances. Validation of TOVS retrievals obtained by the improved initialization inversion ("3I") algorithm revealed substantial deficiencies in the retrievals during the Arctic cold season (Francis 1994). These deficiencies include the misidentification of surface character-

istics, misidentification of clear and cloudy scenes, snow/ice surface temperatures being frequently too warm (by as much as 10°–15°C), and surface temperature inversions being rarely captured. These deficiencies have been addressed by Francis (1994) in an improved version of the 3I algorithm, although errors in the retrieved temperature and humidity profiles are still significant.

3. Cloud characteristics

a. Cloud morphology

The first climatology of cloud amount and type for the Arctic Ocean was compiled by Sverdrup (1933) using data obtained from the *Maud* expedition, where it became apparent that Arctic clouds are difficult to observe and classify. This is particularly true during the cold, dark half of the year for low clouds, which are predominantly crystalline. Hahn et al. (1995) have shown quantitatively that visual observations of cloud cover are hindered at night due to inadequate illumination of the clouds. Moreover, ambiguities in polar cloud classification have hampered the accurate reporting of polar clouds (e.g., Putnins 1970).

Even if a surface observer can "see" the cloud, a quandary is faced about proper terminology for reporting low-level ice crystal clouds (e.g., Hoff and Leaitch 1989). As a result of the ambiguities in cloud classification when applied to the polar regions, low-level ice crystal clouds (commonly referred to as "clear-sky ice crystal precipitation") are likely to go unreported, or to be misreported if observed. The ice crystals may or may not be noted in the present weather code and may be incorrectly coded. In a summary of the climate data for the Canadian Arctic stations, Maxwell (1982) has shown the frequency of low-level ice crystal precipitation (as noted by surface observers in the present weather code) to have maximum values of 0.20 to 0.50 during wintertime, with zero frequency occurrence during the months of June through August. These data in all likelihood underrepresent their frequency of occurrence. Recent observations from the Coordinated Eastern Arctic Experiment (CEAREX) during November 1988 (Overland and Guest 1991) showed measured "clear sky" radiative fluxes to be 10–40 W m^{-2} greater than expected when compared with modeled clear-sky conditions; it was inferred that the additional downwelling flux was associated with lower-tropospheric ice crystals. These measurements make one suspect that there may, in fact, be no such thing as "clear sky" conditions during the polar night or that the definition of clear sky is somewhat arbitrary.

Climatologies of cloud fraction over the Arctic derived primarily from surface observations have been presented by Huschke (1969), Vowinckel (1962), and Gorshkov (1983). Global cloud climatologies (e.g., Beryland and Strokina 1980; Warren et al. 1988; Hahn et al. 1995) have also included meaningful Arctic cloud statistics (for a summary of earlier global cloud climatologies, see Hughes 1984). These climatologies show broad agreement, with a maximum total cloud cover during the summer [as high as 90% according to Huschke (1969)] and minimum during winter (40%–68%). The larger wintertime value of 68% was determined by Hahn et al. (1995) using only moonlit observations. It is noted that none of the surface-based climatologies include the clear-sky ice crystal precipitation. The variability of the total cloud amount over the annual cycle is dominated by low-level clouds, with the frequency of occurrence and total cloud amount increasing to their maximum summertime values over a short transitional period. Curry and Ebert (1992) adjusted the Huschke (1969) cloud climatology to include the clear-sky ice crystal precipitation, based on the surface weather reports summarized by Maxwell (1982), and inferred a total cloud cover of 80% during wintertime. The rationale for this "revised" cloud analysis is to include all cloud particles that interact with radiation, which is arguably more useful for satellite remote sensing and climate modeling studies. Regional variations of Arctic clouds are described by Huschke (1969) and Vowinckel and Orvig (1970), indicating the smallest cloud cover for the Canadian Arctic and the largest wintertime cloud cover for the West Eurasian Arctic (although the wintertime cloud statistics must be viewed as suspect in the absence of the correction for moonlight and inclusion of low-level ice crystal clouds).

Global satellite cloud climatologies have also provided analyses for the Arctic. Satellite cloud datasets that have been analyzed specifically for the Arctic include the U.S. Air Force 3D Nephanalysis (3DNEPH), International Satellite Cloud Climatology Project (ISCCP), *Nimbus 7,* and METEOR. Variability of type and spatial distribution of summer cloudiness in the Arctic basin during late spring and early summer has been examined by Kukla and Robinson (1988) using DMSP satellite data. McGuffie et al. (1988) compared the 3DNEPH with a manual satellite analysis of Arctic clouds and found that the 3DNEPH underestimated significantly the cloud fraction over the Arctic Ocean. Comparison of the ISCCP polar cloud analyses with surface observations (Schweiger and Key 1992) showed that the monthly averaged ISCCP cloud amounts are generally 5%–35% less than the surface-based climatology described by Warren et al. (1980). In a comparison of METEOR, *Nimbus 7,* and ISCCP satellite cloud analyses, Mokhov and Schlesinger (1993) found that METEOR cloudiness was less than both ISCCP and *Nimbus 7* cloudiness during the Arctic winter and ISCCP cloudiness was less than both METEOR and *Nimbus 7* cloudiness during summer. Significant differences exist between surface and satellite climatologies of Arctic clouds (e.g., Schweiger and Key 1993; Rossow et al. 1993; Mokhov and Schles-

inger 1994). A surprising discrepancy between the ISCCP Arctic satellite cloud climatologies and the surface cloud climatologies is that the satellite estimates of wintertime cloud cover over the Arctic Ocean are greater than the surface values (Schweiger and Key 1993; see also Fig. 1). Wilson et al. (1993) have hypothesized that the ISCCP cloud-detection algorithm is picking up a significant portion of the clear-sky ice crystal precipitation that occurs during the cold portion of the year, which was not included in the surface climatology.

As discussed by Raschke (1987) and Raschke et al. (1992), the determination of polar cloudiness using current satellite observations encounters significant obstacles. The polar regions have the lowest surface temperatures and solar illuminations on the earth, and current satellite radiometers are operating near the limit of their performance range. Therefore, the effects of instrument noise, calibration uncertainties, and digitization on radiance accuracy reduces the sensitivity of the satellite radiometers in the polar regions. The visible reflectance of a snow/ice surface is virtually the same as that of a cloud overlying a snow/ice surface. Infrared measurements in the water vapor window provide little useful information since there is little temperature difference between the clouds and the surface. Frequently, in the presence of a temperature inversion, low-level clouds may actually be warmer than the underlying surface. There is also little microwave contrast between the clouds and the underlying snow/ice. Li and Leighton (1991) compared scene identifications obtained from both AVHRR and ERBE measurements over the Arctic and found substantial differences in cloud cover. Significant advances in the remote sensing of clouds in the polar regions have recently been made by including information on spatial coherence (e.g., Ebert 1989; Key 1990; Welch et al. 1992) and temporal coherence (Rossow and Garder 1993) and including near-infrared channels (Key and Barry 1989; Yamanouchi and Kawaguchi 1992; Raschke et al. 1992; Rossow 1995).

Figure 1 shows the annual cycle of total cloud amount from the surface climatology (Warren et al. 1988) and from ISCCP (Rossow et al. 1993) and illustrates the newer surface results for wintertime using the moonlight criterion (Hahn et al. 1995) and the revised ISSCP results using the near-IR channel to provide extra detection, especially in summertime (Rossow 1995). Although the satellite observations still seem to underestimate summertime cloudiness and probably still miss some of the optically thinner ice crystal events, the discrepancies between the surface and satellite observations have been significantly reduced.

Information on cloud depth and heights has been obtained from aerial weather reconnaissance (Henderson 1967; Huschke 1969; Zavarina and Romasheva 1957; Dergach et al. 1960). Lower-tropospheric layers of ice crystals exceeding 3 km in depth in the central Arctic

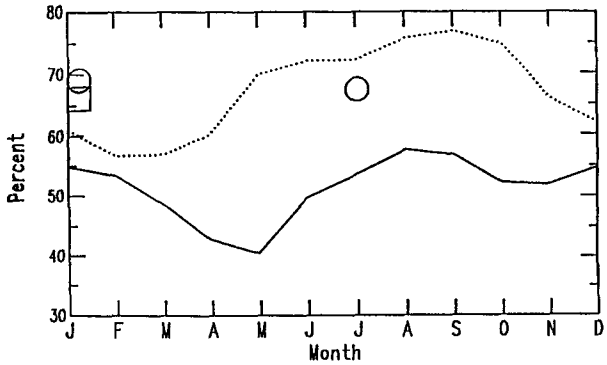

FIG. 1. Mean annual cycle of total cloud cover in percent averaged over 60°–90°N. Solid line is from ISCCP and the dotted line is from surface observations. The two open circles indicate the refined ISCCP estimates using a revised cloud detection algorithm and the open square indicates the refined surface estimates accounting for the effects of varying sky illumination (from Hahn et al. 1994).

have been reported by Witte (1968); shallower layers with depths typically less than 1 km were found during springtime (Curry et al. 1990a). Jayaweera and Ohtake (1973) first described the layered structure of low-level clouds. It appears to be common for summertime Arctic stratus to occur in a number of well-defined layers separated by intervening clear regions that are several hundred meters thick. Herman (1975) and Herman and Goody (1976) cite reports of as many as five simultaneous cloud layers in the lower atmosphere.

b. Microphysical properties

The cloud microphysical properties that determine the cloud radiative properties include: the amount of condensed water, the size and shape of the cloud particles, and the phase of the particles (liquid or ice). This discussion focuses on the lower-tropospheric clouds.

The earliest measurements of cloud microphysical properties over the Arctic Ocean were reported by Koptev and Voskresenskii (1962) and Dergach et al. (1960), which were made from aircraft measurements during the warm portion of the year. Alaskan summertime cloud microphysical properties have been measured from aircraft by Jayaweera and Ohtake (1973). Examination of the data from the summertime Arctic Stratus Experiment in the Beaufort Sea during June 1980 (Herman and Curry 1984; Curry 1986; and Tsay and Jayaweera 1984) showed that the maximum value of liquid water content measured during this experiment was 0.5 g m^{-3}. Values of the measured liquid water paths ranged from 11 to 117 g m^{-2} for low clouds and from 7 to 15 g m^{-2} for middle clouds. Mean droplet radii ranged from 2 to 7 μm and the maximum droplet concentration was 500 cm^{-3}. Droplet equivalent radius (defined to be the average droplet radius weighted by the droplet cross-sectional area) ranged from 3.6 to

11.4 μm, with an average value for low-level clouds being 7.5 μm. In an analysis of the data from the Arctic Stratus Experiment to examine the processes that determine the microphysical properties of the summertime Arctic stratus clouds, Curry (1986) found a significant amount of drizzle associated with a large dispersion of the droplet spectra. The large dispersion was inferred to be associated with the following processes: turbulent fluctuations of vertical velocity; entity entrainment between inhomogeneous parcels; droplet growth near cloud top due to radiative cooling; and coalescence processes due to the long lifetime of these clouds.

The temperatures at which ice crystals occur in the Arctic lower troposphere show a wide range, and the association of phase with temperature is complicated by the fact that falling ice crystals may be observed at levels far away from the level that they were nucleated. From observations reported by Curry et al. (1990a) during April 1983 and 1986, it seems that significant ice crystal nucleation routinely occurs at temperatures as high as $-15°$ to $-20°$C, indicating that the ice particles form by freezing nucleation. Earlier observations by Witte (1968) described one case with condensate that was predominantly liquid at temperatures as low as $-32°$C during December 1967, and Jayaweera and Ohtake (1973) found very few ice crystals at temperatures above $-20°$C during September 1971 and April 1972. Curry et al. (1996) report completely crystalline clouds during October at temperatures as high as $-14°$C. Although general conclusions cannot be drawn due to the small number of observations, it is apparent that there are substantial variations in the phase transition temperature in the Arctic on timescales of days to decades. Curry (1995) has hypothesized that there may be significant differences in the temperature of the phase transition between the spring and autumn seasons arising from differences in aerosol concentration and composition.

Mixed-phase clouds have also been observed in the Arctic boundary layer. Witte (1968) described a case of a very deep mixed-phase cloud that occurred in the presence of a wintertime temperature inversion. Curry and Radke (1994) describe a case observed during April 1983 of a shallow mixed-phase cloud with a top at 600 m. Pinto et al. (1995b) inferred the presence of mixed-phase clouds in March and April 1991 (LEADEX) from the surface radiation flux and ceilometer measurements. Curry et al. (1996) describe mixed phase clouds observed over the Beaufort Sea during the autumn 1994 Beaufort Arctic Storms Experiment (BASE) for cloud temperatures ranging from $-8°$ to $-18°$C.

In the Arctic, the microphysical properties of the lower-tropospheric ice crystals (including clear-sky ice crystal precipitation) have been determined from surface observations (Gotaas and Benson 1965; Ohtake et al. 1982; Leaitch et al. 1984; Trivett et al. 1988), aircraft observations (Witte 1968; Hoff and Leaitch 1989; Curry et al. 1989a, 1989b, 1990a), and lidar (Hoff 1988; Andreas et al. 1990). The reported ice crystal habits range from plates, columnar crystals, irregular and mixed habits, and frozen drops with little diffusional growth. No simple relationship was found to exist between the habit of the lower-tropospheric ice crystals and the local temperature and humidity, with several different ice crystal habits found to coexist in the same ambient air. The size and concentration of ice crystals reported by most investigators is dependent upon the method of measurement. Some measurement techniques cannot examine small crystals, while other techniques result in the fracture of large crystals. Reported sizes range from 8 to 1000 μm, and concentrations exceeding 1000 L^{-1} have been reported. The most comprehensive measurements of ice crystal size distributions were made by Witte (1968). The modal "radius" of the ice crystal size distributions ranged from 10 to 80 μm. Curry and Ebert (1992) determined an ice crystal effective radius to be 40 μm for the lower-tropospheric ice crystals measured by Witte (1968).

Anthropogenic activities input large quantities of water vapor into the atmosphere. "Ice fog" has been defined by Benson (1970) and Bowling (1975) as a form of air pollution that appears at temperatures below $-30°$C in populated regions (notably Fairbanks, Alaska) where topography, combined with strong temperature inversions, causes air to stagnate. Ice fog is composed mainly of small diameter (<20 μm) crystals that have frozen from droplets very rapidly, having so little excess vapor available for further growth that they remained nearly spherical in shape with only a few rudimentary crystal facets (Thuman and Robinson 1954). The source of ice fog is addition of water vapor to the atmosphere that may be associated with hot springs, caribou herds, power plants, and automobiles. Ice fog can reduce visibility to 1/8 mile. These ice crystals that comprise ice fog lack well-developed crystal faces and are not associated with optical effects.

c. *Formation, maintenance, and dissipation processes*

Formation mechanisms of Arctic clouds vary with the region and the characteristics of the underlying surface. Clouds in the marginal ice zone, particularly during autumn when baroclinic effects are strongest, are frequently associated with frontal systems and may be convective in nature (Curry et al. 1990b). Over Alaska, clouds are predominantly stratiform, with increasing amounts of cumuliform clouds in summer (Hahn et al. 1984). Because of the topography, orographic lifting is presumably an important cloud formation mechanism in Alaska. Over the Arctic Ocean, the formation of mid- and upper-level clouds are believed to be closely associated with frontal systems (Curry and Herman 1985). The wintertime maximum and summer-

time minimum of mid- and upper-level clouds is consistent with the association of these clouds with cyclone activity. Low-level clouds, on the other hand, appear to be relatively insensitive to the synoptic situation and form as a result of airmass modification that results as relatively warm, moist air is advected into the polar basin and cools radiatively (Herman and Goody 1976; Curry 1983). During wintertime, it appears that this cloud formation mechanism is operative over Alaska as well (e.g., Gotaas and Benson 1965). The formation of wintertime convective ice crystal plumes associated with leads has been observed by Schnell et al. (1989). Because of their unique characteristics, this discussion will focus on the following boundary-layer cloud types: (i) summertime boundary layer with multiple layers of cloud; (ii) low-level ice crystal clouds and "clear sky" ice crystal precipitation in stable wintertime boundary layers; and (iii) wintertime ice crystal plumes emanating from leads, or cracks, in the sea ice.

1) SUMMERTIME LAYERED CLOUDS

Herman and Goody (1976) considered the formation of the summertime Arctic stratus clouds in the relatively warm and moist continental air as it flows over the pack ice and inferred that condensation is induced in an initially unsaturated air mass due to radiative and diffusive cooling to the colder surface and longwave emission to space. Support for this formation mechanism has been provided by the June 1980 Arctic Stratus Experiment (Curry et al. 1988). The airmass modification results in one or more stratus cloud layers; the top layer may be associated with a shallow mixed layer. Once the stratus/fog becomes optically thick so that cloud-top radiative cooling becomes large, turbulent kinetic energy is produced and vertical mixing occurs, producing more condensation due to adiabatic cooling. While these low-level clouds are not coupled to the underlying surface through turbulence, the term "boundary-layer cloud" may still be applied since these clouds are within the thermal boundary layer.

The multiple layering that is frequently observed to occur in the Arctic summertime boundary layer (Jayaweera and Ohtake 1973; Herman and Goody 1976; Curry et al. 1988) is poorly understood. During summer a shallow, stably stratified cloud layer is often observed beneath an upper cloud-topped mixed layer, with the two cloud layers being turbulently decoupled (Curry et al. 1988). Three hypotheses have been proposed to explain the cloud layering. Herman and Goody (1976) proposed a "greenhouse" mechanism, whereby cloud absorption of solar radiation in the intermediate levels of the cloud causes local evaporation (splitting the cloud deck into two layers) and longwave emission to space from the cloud top and to the colder surface from cloud base maintains the upper and lower cloud layers. Using observations from the Arctic Stratus Experiment, Tsay and Jayaweera (1984) proposed that the upper cloud layer is formed by very weak ascent/entrainment, while the low-level cloud is an advective cloud. McInnes and Curry (1995a,b) suggest that in the presence of a temperature and humidity inversion, radiative cooling will result initially in the formation of a cloud layer near the peak of the inversion, where radiative cooling is the greatest. Further radiative cooling of the cloud layer induces mixing of the cloud, resulting in a cloud base that is cooler than the surface. The air above the surface, which is warmer than both the surface and the upper-level cloud base, cools and condenses, forming the second layer. In principle, this mechanism can be used to explain the formation of more than two layers. It is not clear from our limited observations which of these three mechanisms is really important.

Herman (1975) attributes the persistence of the Arctic summertime clouds to the absence of cloud dissipative processes (e.g., precipitation, radiative heating, convective heating of the boundary layer, large-scale synoptic activity). Modeling results from McInnes and Curry (1995a) suggest that the two layers are most likely to be maintained under conditions of weak, rising motion. By analyzing the cloud microphysical and turbulence data from the Arctic Stratus Experiment, Curry (1986) and Curry et al. (1988) inferred the following: the cloud layer (top layer in the case of a multilayered cloud) is maintained by convection and vertical condensational growth induced by cloud-top radiative cooling; surface evaporation plays little if any role in maintaining the cloud; and cloud-top entrainment has little dissipative effect, especially if the air above the cloud is moist (i.e., humidity inversion).

2) CLEAR-SKY ICE CRYSTAL PRECIPITATION

During wintertime, ice crystals are ubiquitous in the Arctic thermal boundary layer (Curry et al. 1990a). Ice crystal plumes associated with leads may be an important source of these ice clouds (Schnell et al. 1989), while the model of Curry (1983) suggests that low-level ice crystal layers can form through radiative cooling. Using a 1D model, Curry (1983) described the formation of these ice crystals in the context of the modification of a maritime polar air mass advected over the Arctic Ocean and compared the model results with observations described by Gotaas and Benson (1965). As a result of radiative cooling, ice crystals rapidly form in the lower troposphere and slowly settle to the ground. Blanchet and Girard (1995) expanded on this theory, describing a process whereby interactions with sulphate aerosol enhances the condensation and precipitation process in the airmass modification process. Curry (1987) described a positive feedback loop between the formation of condensate in the cooling air and anticyclogenesis: radiative cooling from the condensate enhances anticyclogenesis; and the large-scale meridional circulation associated with the anticyclone

(and the associated subsidence) replenishes the moisture in the layer of condensate because of the humidity inversion, thus enhancing the radiative cooling. These theories for the evolution of wintertime ice crystal clouds remain unvalidated by observations.

3) CLOUDS ASSOCIATED WITH LEADS

During the cold half of the year, strong surface-based convection occurs over leads. Field measurements taken in winter during the AIDJEX Lead Experiment (Andreas et al. 1979; 1980) showed that the turbulent heat fluxes from leads can exceed 400 W m^{-2} for sensible heat and 130 W m^{-2} for the latent heat flux for typical wintertime air–sea temperature differences of 20°–40°C over leads. The surface heat fluxes provide the necessary buoyancy for convection above and downwind of the lead, resulting in vertical and horizontal transport of heat and moisture into the atmosphere. Schnell et al. (1989) illustrated dramatically the possible extent of this transport using airborne infrared lidar observations, where plumes of ice crystals emanating from a wide lead reached heights up to 4 km and were traced 250 km downwind of the lead.

Numerous efforts have been made to model various aspects of vertical transport of heat and moisture into the atmosphere from leads and the ensuing clouds. Pinto et al. (1995a) and Pinto and Curry (1995) used a one-dimensional model with second-order turbulence closure to analyze the thermodynamic, microphysical, and radiative processes occurring in the ice crystal plumes associated with the leads. Modeling results indicated that longwave heating by radiation is as large as by the sensible heat flux convergence in the lowest 20 m of the atmosphere; neglect of radiative transfer, condensation and precipitation processes results in an underestimate in the depth of the affected region of order 10%–20%; and the stability of the atmosphere above the surface temperature inversion is an important control on the internal boundary-layer depth for a shallow surface inversion layer. Major uncertainties remain in our understanding of lead-induced convection and cloud formation, particularly with regards to the cumulative effect of leads on the larger-scale atmospheric heat and moisture budget.

During the colder portion of the year, the existence of thermal streaks aligned in parallel rows over the polar ice cap has been described by Byers and Stringer (1992) and Fett et al. (1994) from satellite infrared imagery. Two types of streaks were distinguished, the first type appears to be associated with roll vortices, having apparent sources at areas of low ice concentration or open water and a typical spacing found of roughly 6 km. The second type consists of alternately warm and cool bands of continuous cloud cover and no easily identifiable point source, with a wavelength of 15–30 km. As pointed out by Fett et al. (1994), the streaks of the second type occur during periods of high wind velocity and may be associated with leads.

4. Cloud–radiative characteristics

a. Summertime

The optical properties of the summertime Arctic stratus clouds are described by Herman and Curry (1984), Curry and Herman (1985), and Tsay et al. (1989) using measurements obtained from the Arctic Stratus Experiment. The single-scattering properties of the cloud drops (e.g., volume extinction coefficient and single scatter albedo) as well as the cloud bulk radiative properties (i.e., reflectance, transmittance, absorptance and emittance) were all found to show significant dependence upon the drop size distribution.

Values of the broadband shortwave optical depth for the summertime Arctic stratus were determined by Herman and Curry (1984) to range from 2 to 24 for low-level clouds and from 2 to 5 for midlevel clouds. Leontyeva and Stamnes (1994) used broadband ground-based measurements of incoming solar irradiance to determine the cloud optical depth for April through August 1988. Mean monthly values of the cloud optical depth ranged from 8 to 20; these values might be slightly higher than the true climatological values since the selected cases were homogeneous and relatively thick.

Using data obtained from AIDJEX, Herman (1977) determined summertime shortwave transmittance, reflectance, and absorptance from aircraft measurements. Herman determined the reflectivity of the cloud plus surface to range from 60%–75% over the entire shortwave spectrum. Herman and Curry (1984), using data from the summertime Arctic Stratus Experiment, determined a "reduced" cloud reflectivity and transmissivity for a hypothetical system with zero surface albedo. Cloud reflectivities ranged from 0.20 to 0.68 and transmissivities ranged from 0.80 to 0.25 over an optical depth range of 2 to 24. In a comparison of cloud absorptivity made with two different radiometers and a radiative transfer model, large discrepancies were found, which is similar to difficulties that have been encountered in determining cloud absorptivity at lower latitudes. Arctic cloud absorptivity has been discussed by Wiscombe (1975) and Herman and Curry (1984).

Emissivity as a function of cloud geometrical thickness was reported by Herman (1980), indicating that clouds less than 320 m thick are not emitting as blackbodies. Bulk cloud emissivities, determined for the summertime Arctic stratus by Curry and Herman (1985), ranged from 0.4 to 1.0. It was found that the liquid water path in Arctic stratus was frequently less than 20 g m^{-2} even during summer and in the range where emissivity is sensitive to drop size distribution. It was further pointed out that the broadband emissivity was not well represented by the window emissivity due to the relative transparency of the water vapor bands outside the window. Spectrally averaged flux mass infrared absorption coefficients were determined for the summertime Arctic stratus to range from 0.03 to 0.18

$m^2\ g^{-1}$ and were found to vary strongly with droplet effective radius. A parameterization was derived of the spectral mass absorption coefficient in terms of the droplet effective radius. The dependence of shortwave radiative properties on cloud dropsize distribution has long been established (e.g., Welch et al. 1980), but the dependence of longwave emissivity on dropsize distribution is typically ignored (e.g., Stephens 1978). This dependence should not be ignored for the Arctic clouds.

In-cloud radiative heating rates were determined by Curry (1986) and Tsay et al. (1989) using data from the summertime Arctic Stratus Experiment and radiative transfer models. Peak shortwave cloud radiative heating rates were determined to be 40°C day^{-1}, with the peak heating rates occurring below cloud top. Peak cloud-top longwave radiative cooling rates were determined to be as large as 165° day^{-1}. Net in-cloud heating rates are generally negative (cooling), although there may be net heating in the lower portion of the cloud associated with the dominance of shortwave heating in the lower part of the cloud and/or a cloud base that is warmer than the surface. Intercloud variations in the magnitude and vertical profile of the heating vary with the magnitude and vertical distribution of the condensed water content and the droplet equivalent radius. Complex vertical variations in the heating rates may arise from the complex vertical cloud and temperature structure. The cloud longwave radiative extinction depths were determined to vary from 32 to 120 m, with the intercloud variation attributed to variations in amounts and vertical distributions of liquid water.

b. *Wintertime*

Observations of the radiative properties of Arctic clouds during seasons other than summer are sparse, particularly for the wintertime situation with low-level crystalline clouds. Because of the virtual absence of sunlight, the dominant radiative effect of clouds during wintertime is on the longwave radiative fluxes. The only in situ observations of radiative fluxes in wintertime Arctic clouds that we are aware of are those reported by Witte (1968) for the 8–14 μm spectral region. Calculations using the ice crystal concentrations and size spectra observed by Witte (1968) were recently made by Curry et al. (1990a), showing perturbations to the infrared surface flux by the clear-sky ice crystal precipitation to be as large as 80 W m^{-2}. Values of the visible optical depth for the ice crystal layers were determined to range from 5 to 21 for wintertime and from 0.03 to 3 for springtime. Using an infrared radiative transfer model and observed microphysical and thermal characteristics, the longwave radiative perturbation associated with the ice crystals (relative to clear air) was determined to be as large as 3°C day^{-1}.

Pinto et al. (1995b) determined cloud optical depths during LEADEX (March–April 1992), from surface-based shortwave radiation measurements. A mean shortwave optical depth was determined to range from 5.1 to 6.7, depending on the assumptions made about cloud phase. Key et al. (1994) used the 0.9 and 3.7 μm wavelengths of AVHRR to retrieve cloud optical depth and effective radius during LEADEX. Retrieved optical depth values ranged from 1 to 16, and values of the effective radius ranged from 4 to 8 μm.

c. *Annual cycle*

Direct observations of cloud optical depth over the annual cycle are not available. Therefore, two studies are described here, including an observationally constrained model simulation and analysis of satellite data.

The annual cycle of cloud–radiative properties was derived by Curry and Ebert (1992) using a 1D coupled atmosphere–sea ice model. Using observed climatologies of surface radiation fluxes and values of the top-of-atmosphere (TOA) fluxes derived from ERBE observations, the annual cycle of cloud characteristics were determined that, when input into a radiative transfer model, would yield the observed components of the surface and TOA radiative fluxes. Where possible, the cloud characteristics were constrained by observations. The monthly averaged values of cloud (visible) optical depth, weighted by cloud fraction, were determined to range from 2 during winter to a summertime maximum of 8. The values of optical depth for individual cloud layers, when present, ranged from 0.5 during winter for mid- and high-level clouds to 8 for summertime stratus clouds. The average optical depth of the lower-tropospheric ice crystal clouds during winter was determined to be 3. The monthly averaged bulk cloud infrared emissivities ranged from 0.2 to 0.4 for high clouds, averaged 0.9 for mid- and low-level clouds during summer, and were as high as 0.9 during midwinter for the lower-tropospheric ice crystal clouds.

Cloud optical depth has been determined from satellite using the ISCCP analysis by Rossow and Garder (1993). Despite current uncertainties in satellite determinations of cloud radiative characteristics in polar regions, some qualitative features of these results are consistent with other available information. In the Arctic, the ISCCP analysis is most reliable in summertime when liquid water clouds are more prevalent and the surface reflectivity is lower; the average summertime optical thickness is about 10–15 at 0.6-μm wavelength, although this average is somewhat uncertain because of the missed low-level clouds. Spring and autumn cloud optical thicknesses determined from ISCCP are much larger than the summertime values (about 40–60) but are significantly overestimated by use of a spherical particle scattering phase function instead of one that more closely resembles that for ice crystals (cf. Minnis et al. 1993) and because the retrieval of optical thickness from visible reflectance at very low solar zenith angles has two solutions. There are insuf-

ficient observations to determine whether in reality spring and autumn optical depths exceed the summertime values.

5. Radiative properties of the Arctic atmosphere

The radiation environment of the Arctic is dominated by the absence of shortwave radiation for a significant portion of the year. During midsummer, the day length is 24 hours, although the solar zenith angle never gets below 60° at the highest latitudes. The minimum solar zenith angle is only 43° at the Arctic Circle at noon of the summer solstice and increases to 66.5° at the pole.

a. Clear sky

Low temperatures, low moisture content, and the vertical asymmetry associated with inversions make infrared radiative transfer in the cold Arctic air markedly different from transfer in lower latitudes. Radiative energy exchange in cold Arctic air is concentrated in different parts of the infrared spectrum from exchange in warmer, moister air. In the coldest air masses, the opacity of the water vapor rotation band decreases due to the small amount of water vapor. In addition, the blackbody intensity maximum shifts toward the low-frequency rotation band as temperature decreases. As a result, the proportion of cooling from the water vapor rotation band is much greater than air at lower latitudes. Because of the low moisture content, radiative exchange due to CO_2 becomes increasingly important relative to that of water vapor. Exchange in the water vapor continuum is negligible in the absence of condensate.

Ellingson et al. (1996; manuscript submitted to *J. Climate*) discuss the importance of the water vapor rotation band, 400–600 cm^{-1}, in Arctic radiative transfer. At low water vapor contents typical of the Arctic winter, a "dirty window" is opened in the spectral region 400–600 cm^{-1}, and the maximum lower-tropospheric cooling rates occur in this spectral region (instead of in the water vapor window in the spectral region 800–1250 cm^{-1}). Line by line radiative transfer calculations show significant disagreement with spectrally detailed observations, implying a significant uncertainty in our ability to accurately model clear-sky radiative fluxes in the Arctic.

Curry et al. (1995b) examined the impact of atmospheric temperature and humidity on surface and TOA clear-sky radiative fluxes by using a spectral radiative transfer model, in the context of the normalized greenhouse factor G, which is defined to be the ratio of the upwelling longwave flux emitted from the surface to the upwelling longwave flux at the top of the atmosphere (following Stephens and Greenwald 1991; Webb et al. 1993). Using a simple emissivity model, Stephens and Greenwald (1991) proposed that G is linearly related to precipitable water, which was borne out by satellite observations in oceanic regions. The linear relationship was assumed to arise from the fact that changes in emitted radiation to space that result from changing water vapor amount occur primarily in the transparent spectral regions of the water vapor absorption spectrum. A nonlinear relationship between the clear-sky greenhouse effect and precipitable water was found in the Arctic by Curry et al. (1995b) because changes in emitted radiation to space with changing water vapor amount arise from radiative transfer in the normally opaque portions of the water vapor rotation band and vibration–rotation band. The clear-sky greenhouse effect is also affected by temperature inversions and is smaller for a stronger inversion.

The clear-sky ratio of direct to diffuse shortwave radiation was measured by Herman and Curry (1984) during the summertime Arctic Stratus Experiment. The observed (clear-sky) ratios varied from 0.12 to 0.30. Model calculations suggest that varying amounts of aerosol can explain the observed variations in the direct/diffuse ratio.

b. Surface fluxes

The most comprehensive in situ measurements of the surface radiation balance over the Arctic Ocean are the Russian measurements made from drifting ice stations (e.g., Marshunova 1961; Marshunova and Chernigovsky 1966; Gavrilova 1963; Vowinckel and Orvig 1964). These early observations are assessed and interpreted by Fletcher (1965). The entire time series of Russian surface radiation measurements is summarized by Marshunova and Mishin (1995) using data from 1950 to 1991. These measurements have been supplemented by data from some field experiments (e.g., Francis et al. 1991; Steffen and DeMaria 1995; Ruffieux et al. 1995). Outside the central Arctic, Ohmura and Gilgen (1991) describe radiation measurements made in the coastal Arctic, Maykut and Church (1973) and Wendler and Eaton (1990) describe the radiation climate at Barrow, Alaska, and ten years of radiation data at Resolute, Canada, are described by Cogley and Henderson-Sellers (1985).

As shown in Figs. 2–4, longwave (LW) radiation dominates the surface radiation balance in the polar regions during much of the year. Incoming shortwave (SW) radiation is negligible during late fall, winter, and early spring, and even during midsummer the incoming shortwave radiation is only slightly greater than the incoming longwave radiation. The annual total incoming longwave is more than double the incoming shortwave radiation. This arises primarily from the high solar zenith angle at high latitudes. Maykut (1986) summarizes different empirical relationships used in the Arctic to determine the components of the incoming radiation that reaches the surface based on surface observations and solar geometry. Wendler and Eaton (1990) determined the net surface radiation balance at Barrow to be positive only during June, July, and August, coinciding with the snow-free months.

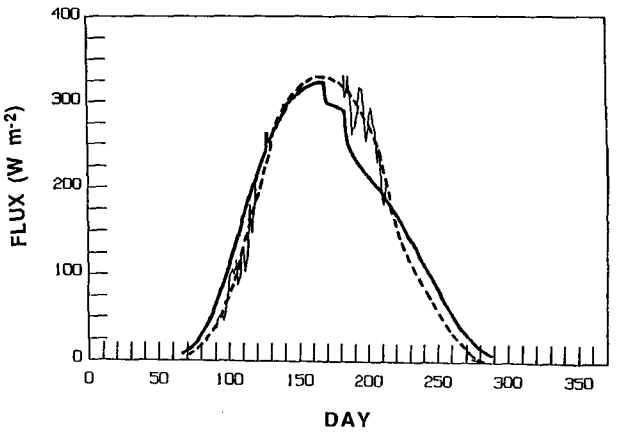

FIG. 2. Annual cycle of downwelling surface SW radiation flux for 80°N. Curry and Ebert (1992) analysis (heavy solid); Rossow and Zhang (1995) analysis based on ISCCP for four months in 1985 (thin solid); smoothed annual cycle fit to the four-month ISCCP analysis (dash).

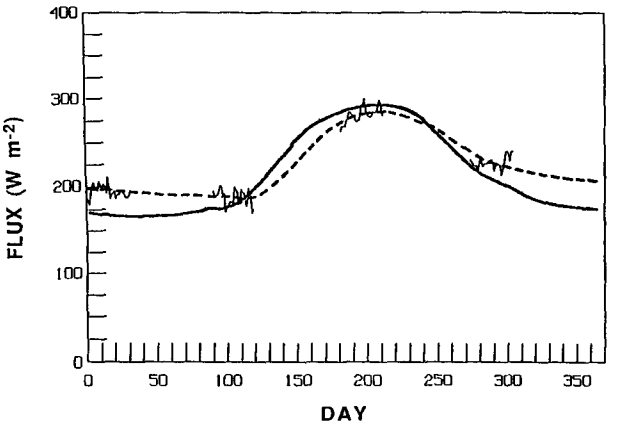

FIG. 3. As in Fig. 2 but for the annual cycle of downwelling surface LW radiation flux for 80°N.

An obvious advantage of satellite-derived surface radiation fluxes is the potential to address the issue of spatial variability, which cannot be done with anything approaching the past and present surface-based observations. Surface radiative fluxes were computed by Schweiger and Key (1994) over the Arctic Ocean (north of 62.5°N) using the ISCCP cloud dataset. Comparison of the satellite-derived surface fluxes using ISCCP clouds with the Curry and Ebert (1992) analysis (for 80°N) are shown in Figs. 2–4, where the surface radiative fluxes were determined following Rossow and Zhang (1995). Figure 2 compares the annual cycle of downwelling SW flux at the surface inferred by Curry and Ebert (1992) and Rossow and Zhang (1995); although there is agreement to within 10–20 W m^{-2} in April, the ISCCP values in July are about 40 W m^{-2} higher than found by Curry and Ebert, primarily because of the much lower summertime cloud cover in the ISCCP analysis. However, the higher surface albedo in the ISCCP analysis produces almost the same net SW flux at the surface as found by Curry and Ebert. Figure 3 shows the downwelling LW fluxes at the surface. The agreement in July is within about 10 W m^{-2} despite the large differences in cloud cover because the clouds included in the ISCCP analysis, although they have higher tops than the clouds that are missed, have about the same base heights in these calculations. In wintertime, the ISCCP analysis overestimates the downwelling LW flux relative to Curry and Ebert because the clouds have much higher optical thicknesses. However, in the ISCCP analysis the surface temperatures, which are warmer than Curry and Ebert, produce larger upwelling LW fluxes so that the net surface fluxes in both Curry and Ebert (1992) and Rossow and Zhang (1995) agree to within about 10 W m^{-2} (Fig. 4). That the surface net radiation flux is only weakly negative (cooling) is a consequence of the significant LW heating of the surface by the atmosphere.

A critical feature of the net surface radiation balance is the surface albedo. Spectral albedos and wavelength-integrated albedos observed over different types of ice and snow have been described by Langleben (1969, 1971), Grenfell and Maykut (1977), Perovich and Grenfell (1981), Grenfell and Perovich (1984), Perovich et al. (1986), and Perovich (1994). Modeled surface albedos over ice are described by Grenfell (1983), Shine and Henderson-Sellers (1985), Buckley and Trodahl (1987), Jin et al. (1994), and Warren and Wiscombe (1980) and over snow by Wiscombe and Warren (1980). Snow albedo has been found to be sensitive to grain size and amount of soot. Ice albedos have been found to be sensitive to surface conditions, to air bubble density in the ice, and to the amount and distribution of brine in the ice interior. Ebert and Curry (1993) synthesized these results in a surface albedo

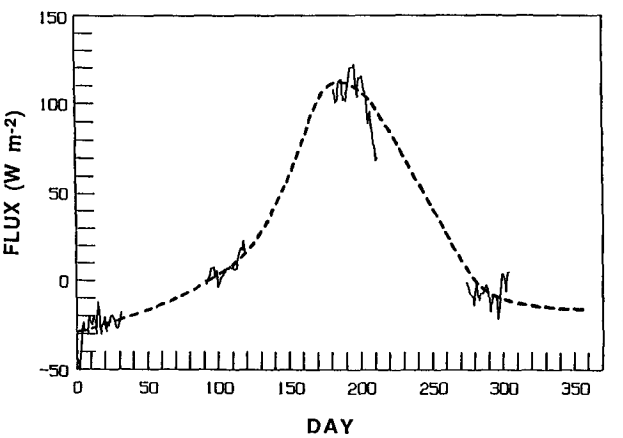

FIG. 4. As in Fig. 2 but for the annual cycle of net surface radiation flux for 80°N.

parameterization that considers both the spectral variation in albedo as well as its dependence on solar zenith angle. Five surface types are included: new snow, melting snow, bare ice, meltwater ponds, and open water, for each of four intervals in the solar spectrum. The annual cycle of Arctic Ocean broadband surface albedo ranges from approximately 0.83 during winter, when the surface is largely snow covered, to a summertime minimum of 0.48 when the surface is a mixture of bare ice, melt ponds, and open leads.

Clouds influence the surface albedo by selectively absorbing solar radiation at wavelengths greater than about 0.7 μm. Because the spectral reflectivities of snow and ice are greater in the visible region than in the near-infrared, the surface albedo under clouds exceeds the clear-sky value. This has been clearly demonstrated by measurements (e.g., Grenfell and Maykut 1977; Grenfell and Perovich 1984) and modeling studies (e.g., Choudhury and Chang 1981; Shine and Henderson-Sellers 1985). In addition, clouds alter the distribution of the solar flux between direct and diffuse components. This can be important for surface types whose reflection characteristics are not Lambertian. In particular, the direct albedos of dry snow and open water depend significantly on the angle of the sun (Wiscombe and Warren 1980; Briegleb et al. 1986).

Bidirectional reflectance distribution, which is the angular distribution of reflected radiance as a function of solar incidence angle, has been studied for snow and ice by Dirmhirn and Eaton (1975), Kuhn (1985), Steffen (1987), Dozier et al. (1988), Schlosser (1988), and Perovich (1991, 1994). Perovich (1994) concluded from observations from the visible to the near-infrared that at most angles, reflectance has the same spectral shape as albedo, at 30° zenith reflectance is for the most part azimuthally isotropic, and at 60° zenith there is a significant specular component at 0° azimuth especially for the bare ice cases. Light reflected at 60° zenith angle was strongly polarized. Light reflected from snow-free ice was generally strongly polarized, with the degree of polarization increasing with wavelength.

Satellite determination of areally averaged Arctic ice and snow albedo has been made by Robinson et al. (1992) using the Operational Line Scan (OLS) imagery from the Defense Meteorological Satellite Program and Rossow and Schiffer (1991) using the ISCCP analyses. Schweiger et al. (1993) analyzed these two datasets and found the spatial patterns to be in general agreement, although the ISCCP values were systematically lower by 0.10. The errors in the ISCCP surface albedo determination are believed to be associated with inadequacies in the cloud threshold in the earlier ISCCP analyses. Inadequate calibration of the OLS radiances make this dataset unsuitable for surface albedo determination. Using AVHRR data with manual cloud detection, Lindsay and Rothrock (1994) determined monthly averaged surface albedo of central Arctic sea ice to range from 0.73 in April to 0.42 in August. Uncertainties in instantaneous, area-averaged albedos determined by Lindsay and Rothrock of 0.13, 0.04, and 0.08 are associated with uncertainties regarding aerosols, ozone, and water vapor, respectively.

The effect of the high surface albedo on incoming radiation was first reported by Nansen (1897), who utilized the "dark" underside of stratus clouds to navigate to open water. Catchpole and Moodie (1971), Wendler (1972), Wiscombe (1975), Shine (1984), Wendler and Eaton (1990), and Pinto and Curry (1996) showed the increase of downwelling shortwave radiation in the presence of clouds using both observations and model calculations. This increase in downwelling surface shortwave radiation arises from the multiple reflections between the atmosphere (particularly clouds) and the highly reflecting snow/ice surface. Shine (1984) showed that the error of not including multiple reflections would result in the underestimation of the modeled incoming surface shortwave radiation flux by 50%.

Snow emits very nearly as a blackbody. Directional surface emissivities for snow are described by Dozier and Warren (1982). The relationship between surface temperature and surface albedo is important for interpreting ice–albedo feedback, and such a relationship is commonly used in climate model parameterizations. Sellers (1969), Ledley (1991), and Harvey (1988) assumed that the surface albedo is a linear function of surface temperature. While such a relationship captures the gross changes associated with an ice versus ice-free state, this relationship is not simple in the Arctic (Lindsay and Rothrock 1994; Curry et al. 1995a). During the summer melt season, surface temperature remains constant while surface albedo decreases. During the low-sun months, surface albedo remains relatively constant while surface temperature varies with insolation. During the transition seasons, surface albedo decreases as surface temperature increases.

c. *Top of atmosphere fluxes and atmospheric absorption*

Schweiger and Key (1994) showed that ISCCP fluxes at the top of the atmosphere (TOA) are in excellent agreement with ERBE measurements. Figure 5 shows the annual cycle of upwelling SW flux inferred by Curry and Ebert (1992), which is constrained by ERBE results, compared with values calculated from ISCCP for April and July 1985 (following Rossow and Zhang 1995). Quantitative agreement is good, within about 10–15 W m^{-2}. Figure 6 shows the annual cycles of upwelling LW fluxes; again there is excellent agreement to within about 10 W m^{-2}. Only in July is the net top-of-atmosphere flux positive (heating).

The North Polar area undergoes an extreme seasonal variation in solar heating, from a summertime peak of about 250 W m^{-2} to zero in wintertime (Nakamura and Oort 1988; Rossow and Zhang 1995), which partially

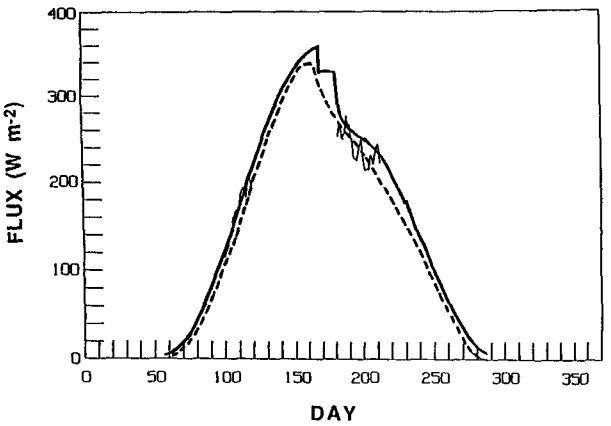

FIG. 5. As in Fig. 2 but for the annual cycle of TOA SW radiation flux for 80°N.

offsets the variations of the longwave cooling of the atmosphere with temperature. Even though longwave cooling peaks in July, shortwave absorption also peaks then, so that the summertime is not the season of maximum atmospheric cooling. In contrast, even though large amount of cloud enhances the longwave cooling in January, much lower temperatures reduce the longwave cooling generally so that wintertime is not the season of minimum cooling. The atmospheric cooling is nearly constant over the year, despite an almost 30°C variation in temperature. Moreover, peak cooling occurs in autumn and minimum cooling occurs in spring through the complex interplay of atmospheric temperatures and cloud properties.

The atmospheric cooling is increased by clouds and the surface is more strongly heated by the atmosphere in the presence of clouds (Rossow and Zhang 1995). In summertime, cloud also decreases the absorption of solar radiation at the surface and the cloud effect on the net atmospheric flux (cooling) is reduced by almost half to about -20 W m^{-2} by shortwave absorption in the clouds. Adding clouds to the wintertime polar air increases the net longwave flux at the top of the atmosphere by about 50% to about -140 W m^{-2} (cooling). The clear-sky atmospheric net radiation is predominantly longwave cooling; the net longwave flux out of the atmosphere is more than 100 W m^{-2}. The seasonal cycle of atmospheric temperature causes larger longwave cooling in summertime than in wintertime; however, the total clear-sky cooling is offset in summertime by shortwave absorption (Rossow and Zhang 1995). This occurs despite low water vapor abundances because of longer daylight and the very long slant path of sunlight. This interaction produces a unique situation where the maximum atmospheric cooling rates appear in the transitional seasons when greater temperatures enhance longwave cooling but shortwave heating is minimal.

d. Cloud radiative forcing

Ramanathan et al. (1989) defined the cloud longwave (C_{LW}) and shortwave (C_{SW}) radiative forcing to be

$$C_{LW} = F(A_c) - F(0)$$
$$C_{SW} = Q(A_c) - Q(0), \quad (1)$$

where A_c is the cloud fraction and Q and F are the shortwave and longwave fluxes, respectively (note that here the radiative fluxes are defined to be positive downwards). The values of cloud forcing are negative for cooling and positive for warming. The net cloud forcing, C, is the sum

$$C = C_{LW} + C_{SW}. \quad (2)$$

The cloud forcing may be determined either at the top of the atmosphere or at the surface. Herman (1975) did an early cloud forcing calculation using Arctic surface radiation data tabulated by Vowinckel and Orvig (1964). Herman determined that clouds have a net warming effect on the surface for all months except July.

Using a 1D coupled model of the atmosphere and sea ice system, Curry and Ebert (1992) evaluated the cloud radiative forcing at the top of the atmosphere and the surface (Figs. 7–10) for a latitude of 80°N. Strong seasonal variations were determined for TOA C_{SW}, with little variation in C_{LW}, resulting in a strong annual variation in C. Total TOA cloud forcing is positive only from mid-September through mid-October, with values near zero during winter and large negative values during midsummer. Strong seasonal variations are also determined for surface C_{SW}, with little variation in C_{LW}, resulting in a strong annual variation in C. Values of surface C are positive except for two weeks in midsummer. Over the course of the year, clouds have a net warming effect on the surface in the Arctic; this is in

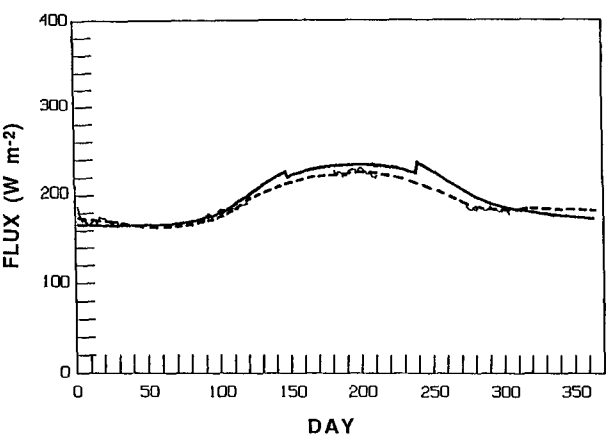

FIG. 6. As in Fig. 2 but for the annual cycle of TOA LW radiation flux for 80°N.

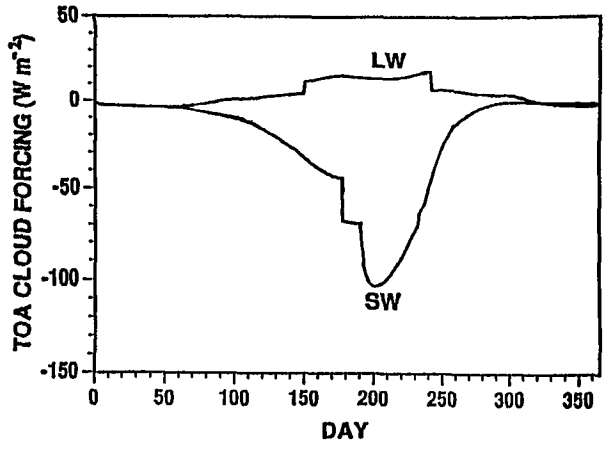

FIG. 7. Annual cycle of TOA longwave and shortwave cloud forcing as determined by Curry and Ebert (1992) for 80°N.

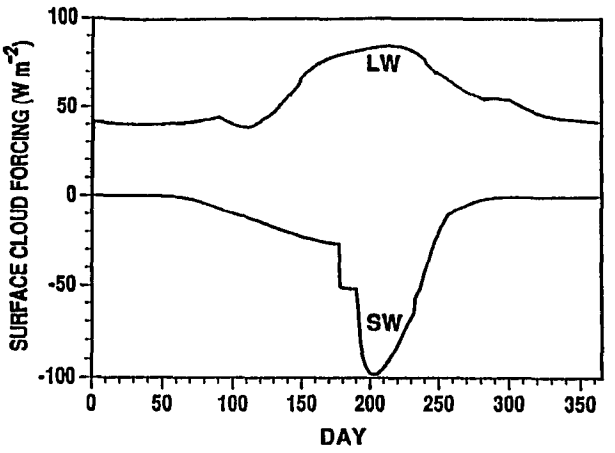

FIG. 9. Annual cycle of surface longwave and shortwave cloud forcing as determined by Curry and Ebert (1992) for 80°N.

contrast to lower latitudes, where clouds have a net cooling effect. This difference arises due to absence of solar radiation during the polar night and due to the high surface albedo of the sea ice. It is noted here that C_{SW} and thus C are strongly sensitive to the value of surface albedo.

Satellite-derived values of the TOA cloud forcing have been made by Ramanathan et al. (1989), Li and Leighton (1991), and Schweiger and Key (1994). Using ERBE data, Ramanathan et al. (1989) show positive values of TOA C_{SW} over the Arctic. The positive values determined by Ramanathan et al. probably reflect difficulties that the cloud detection algorithm has at picking up low clouds in the Arctic, particularly those that are nearly as warm as or warmer than the surface. This result has raised the question as to whether or not the addition of clouds to the atmospheric column can decrease the TOA albedo over bright snow-covered surfaces (e.g., Harrison et al. 1990). Nemesure et al. (1994) collocated ERBE shortwave pixel measurements with surface insolation measurements made at snow-covered locations and found a negative correlation between TOA albedo and surface insolation. Because increased cloudiness acts to reduce surface insolation, these negative correlations demonstrate that clouds increase the TOA albedo over snow-covered surfaces. Shortwave values of TOA cloud forcing during July reported by Li and Leighton show substantial discrepancies between values determined using the AVHRR and the ERBE data (note that the AVHRR scene identification was used for both determinations). The ERBE values of cloud forcing are generally in close agreement with the Curry and Ebert (1992) values. Schweiger and Key (1994) determined cloud radiative forcing using 7 years of ISSCP cloud analyses for the ocean areas north of 62.5°N. The latitudinal variation of the ISCCP-derived TOA cloud radiative forcing for July shows good agreement with the

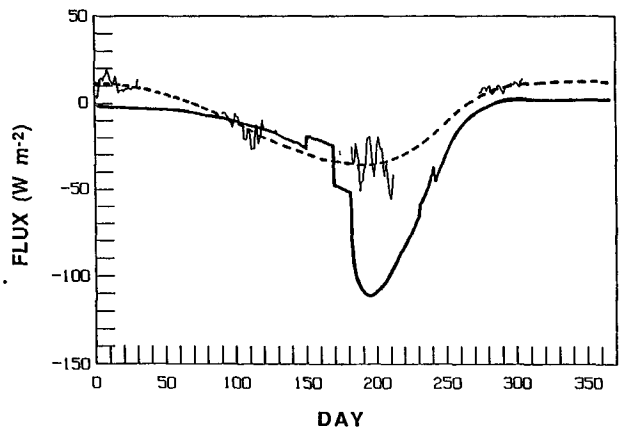

FIG. 8. As in Fig. 2 but for the annual cycle of net TOA cloud forcing for 80°N.

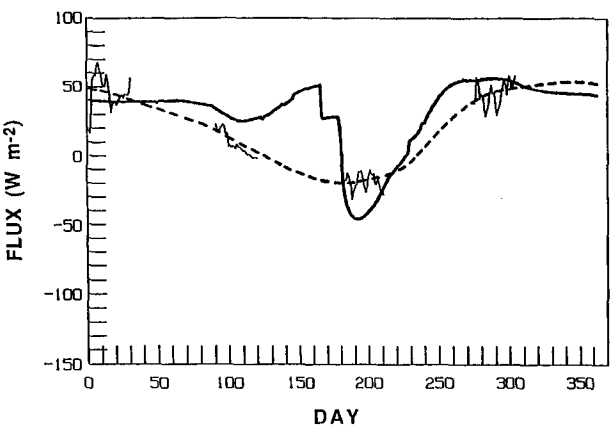

FIG. 10. As in Fig. 2 but for the annual cycle of net surface cloud forcing for 80°N.

AVHRR-derived values presented by Li and Leighton (1991).

We use the ISCCP datasets and the method of Zhang et al. (1995) to provide another estimate of cloud radiative forcing. Figures 8 and 10 compare the net TOA and surface cloud forcing (respectively) for the Ebert and Curry (1992) analysis and the ISCCP analysis. The two analyses generally agree that clouds reduce the wintertime net cooling of the surface by 40–50 W m^{-2} to only 20–30 W m^{-2} and decrease the summertime heating by solar radiation by 20–40 W m^{-2} to about 100 W m^{-2}. The summertime differences arise because of the differing cloud amounts and surface albedos. Although the quantitative agreement of cloud forcing is better in wintertime, which is dominated by LW fluxes, the ISCCP results suggest that clouds decrease slightly the LW cooling. The differences between the two results highlight the need for more accurate measurements of the properties of the atmosphere, surface, and clouds in the Arctic, but also illustrate how small the cloud effects are since the assumed cloud properties, particularly cloud cover and optical thickness, are very different in these two results. Figures 7–10 make another point, that seemingly small differences of these two reconstructions of the surfaces fluxes can be important; it shows that even though both analyses also produce consistent radiative fluxes at the top of the atmosphere, their inferred cloud effects are very different. Hence, even though the surface flux effects are similar, the implied effects on the atmosphere are different, which would imply different forcing for the atmospheric circulation. To work out the complete energy balance and examine feedback processes, we need more detailed measurements of the complete annual cycle of cloud properties taken together with measurements of the variations of atmospheric and surface characteristics and radiation fluxes.

6. Aerosol effects

Arctic aerosol (and aerosol precursors) is derived from both maritime and terrestrial sources and includes an anthropogenic component. Bigg (1980) reported the following aerosol characteristics obtained from measurements taken at Barrow: (i) sulfuric acid is the dominant winter aerosol and winter size distributions are remarkably constant; (ii) in spring the sulfuric acid particles were more numerous and larger than in winter and contained a much greater proportion of ammonium sulfate than in winter; (iii) over one-half of the acid particles contained insoluble inclusions (including clay); and (iv) a sea salt component the aerosol is present. Shaw and Wendler (1972) noted a large springtime maximum in turbidity in the Alaskan Arctic (commonly referred to as "arctic haze"), which was shown to be pollution-derived (Rahn et al. 1977). In addition to a large sulfate component to the springtime aerosol, there is a significant black carbon component (e.g., Rosen et al. 1981; Clarke and Noone 1985). For a review of Arctic air pollution, see Stonehouse (1986) and Barrie (1986). Based on a variety of evidence, it has been concluded that the pollution originates in the midlatitudes of the North American and Eurasian continents, with the most important transport pathways coming from Eurasia. The transport mechanisms of pollution from the midlatitudes to the Arctic are particularly efficient during winter and spring, when the principal industrial centers are north of the polar front. The wintertime Arctic pollution aerosol has been observed to have a long residence time, which has been hypothesized to occur as a result of weak pollutant transformation and removal rates that are caused by the radiative and thermodynamic characteristics of the Arctic winter troposphere.

Ferek et al. (1995) examined dimethyl sulfide (DMS), sulfur dioxide, non-sea-salt sulfate, and various aerosol properties near Alaska, using surface and aircraft measurements. DMS concentrations in the Arctic atmosphere ranged from a few pptv in spring and fall to a few tens of pptv during summer. DMS concentrations measured below the ice and in ice-algae and kelp cultures showed concentrations comparable to those in other oceanic regions. These measurements indicate that the Arctic Ocean is potentially a substantial source of atmospheric DMS, particularly during summer. The seasonal cycle of atmospheric DMS closely resembles that of fine particles, indicating that DMS is likely an important precursor to the type of particles that comprise the background Arctic aerosol in summertime.

High-latitude volcanic eruptions have been shown by Vedder et al. (1987) to lead to concentrations poleward of the source. Whereas in midlatitudes, the long-term radiative effect of the Mt. St. Helens May 1980 eruption was minor; enhanced optical depth of four times the climatic background value was observed in north polar regions by McCormick and Trepte (1987) throughout 1980 and 1981.

The impact of aerosols on the Arctic climate arises from perturbations to the radiative balance. The "direct" effects of aerosols on the radiative balance arise from the perturbations to the radiative fluxes associated with the absorption and scattering of radiation by the aerosol itself. This is in contrast to the "indirect" effects of aerosols on the radiative fluxes that arise from the impact of aerosols on cloud microphysical (and optical) properties. Considerable interest has recently been generated by the studies of Shaw (1983, 1987) and Charlson et al. (1992), suggesting that the direct and indirect radiative effects of aerosols in the troposphere may be sufficient on a global basis to offset the radiative effects of increasing greenhouse gases.

a. "Direct" effects on radiation balance

"Dry" aerosol, without any water uptake, scatters shortwave solar radiation and the carbonaceous com-

ponents of the aerosol absorb solar radiation. The vertical and horizontal shortwave optical depth of the springtime tropospheric aerosol was determined using a sun photometer by Dutton et al. (1991) to range from 0.1 to 0.7. The aerosol extinction obtained from these values averaged 0.03 km^{-1}. Aerosol absorption coefficient (associated with the elemental carbon) was determined by Patterson et al. (1982) to be 0.002 km^{-1}. The dry aerosol particles are too small to interact with the infrared thermal radiation (e.g., Shaw and Stamnes 1980). However, Blanchet and List (1987) have pointed out the importance of considering water uptake by deliquescent aerosols in determining the radiative effects of aerosols, which may substantially increase the size of the aerosol particles. Blanchet and List found that at high relative humidities, the infrared optical depth of deliquescent aerosols may be as large as the visible optical depth.

Early estimates by Shaw and Stamnes (1980) indicated atmospheric shortwave radiative heating rates as high as 1°C day^{-1} directly due to the (dry) Arctic pollution aerosol. More recent estimates made by Valero and Ackerman (1986) indicate atmospheric heating rates associated with the aerosol to be between 0.02 to 0.19°C day^{-1}. Because of the complexity of the vertical temperature and humidity structure in the Arctic and the highly reflecting underlying snow/ice surface, the direct radiative response to the aerosols can be complex. Chylek and Coakely (1973) discussed the effect of surface albedo on atmospheric heating by aerosols and showed that a diffusing aerosol layer over a dark surface increases the reflectivity of the system (cooling effect), while an absorbing aerosol like soot over a bright snow surface reduces the reflectivity of the surface–atmosphere column (warming effect). McCracken et al. (1986) and Emery et al. (1992) have suggested that the atmospheric shortwave heating by the aerosols can enhance the downwelling infrared radiation received at the surface and may overcompensate for the depletion of shortwave radiation at the surface. The amount of compensation depends on the vertical distribution of the aerosol, the emissivity of the atmosphere, and the albedo of the surface. Emery et al. (1992) showed that the perturbation to the radiative fluxes depended strongly on the assumptions made about the response of the atmospheric humidity to the warming: if the relative humidity remains constant, then the surface warms and, if the specific humidity remains constant, then the surface cools. Blanchet and List (1987) have further hypothesized that contamination of the Arctic snow surface by soot and the reduction of snow albedo by increasing the diffuse radiation component in haze conditions will increase the absorption of solar radiation at the ground and can compensate for the attenuation of incident radiation at the surface from the presence of Arctic aerosol (e.g., Warren and Wiscombe 1980).

Clearly, the direct radiative effects of aerosols on the Arctic radiation balance are very complex. The absorption and backscattering of solar radiation by aerosol will have a cooling effect on the surface, which will at least be partly countered by the increased diffuse component of shortwave radiation and the decreased surface albedo. The infrared emission to the surface will be enhanced by the warmed atmosphere and by infrared emission from deliquescent aerosol, although this warming depends on a relatively high atmospheric relative humidity and also advection from lower latitudes. On balance, the net direct perturbation to the surface radiation balance by the aerosol is likely to be a small, positive warming. It is noted here that this is in contrast to the surface cooling expected globally as a result of aerosols. This results from the temperature and humidity inversions and the highly reflecting snow/ice surface that characterize the Arctic climate.

b. Cloud–aerosol interactions

Water vapor condenses in the atmosphere to form liquid water drops by heterogeneous nucleation on certain types of aerosol particles, particularly water-soluble particles or large particles, which are referred to as cloud condensation nuclei (CCN). Aerosol particles that are insoluble in water also play a role in the nucleation of ice particles in the atmosphere; such aerosols are referred to as ice-forming nuclei (IFN).

Radke et al. (1976) describe aircraft measurements of CCN that were made near Barrow during March, with an average CCN concentration of 90 cm^{-3} CCN at 1% supersaturation. Aircraft in situ CCN values measured by Rathore (1983) during the Arctic Stratus Experiment were five times higher than values reported by Radke et al. (1976), and the importance of gas to particle conversions occurring in the Arctic stratus clouds was highlighted. Radke and Hobbs (1969) suggested that this enhancement of CCN activity in clouds is due to the oxidation of SO_2 to form sulfate in cloud droplets. Any material formed by chemical reactions in the droplets that precipitates out of solution when the drop evaporates may either become a new aerosol particle or increase the size of an existing aerosol particle. The oxidants responsible for sulfate production in clouds include hydrogen peroxide, ozone, and oxygen.

The sulfate component of the Arctic pollution aerosol is a particularly good CCN. Heintzenberg et al. (1986) and Shaw (1986) have suggested that the Arctic pollution aerosol may modify cloud water nucleation processes in the Arctic. All other factors remaining the same, increasing amounts of CCN will result in a larger number of water droplets with smaller sizes. Albrecht (1989) and Twomey (1991) have further suggested that not only would drop size decrease as a result of increased CCN, but the total liquid water content of the cloud would increase due to decreasing efficiency of the precipitation process. The lifetime of an individ-

ual cloud might increase, thus increasing the areal coverage of the clouds. In assessing the impact of CCN on the drop size distribution, it should be kept in mind that cloud dynamics (particularly turbulence and entrainment) influences drop size distribution as well (e.g., Sedunov 1974; Baker and Latham 1979; Telford and Chai 1980; Telford and Wagner 1981). However, due to the statically stable Arctic environment and low levels of turbulence in the Arctic clouds, it is hypothesized by Curry (1995) that cloud dynamical effects are of secondary importance and that the principal determinant of the drop size distribution in Arctic clouds is the background air chemistry and CCN characteristics.

In comparing the observations from the Arctic Stratus Experiment with earlier measurements, Curry and Ebert (1990) found that the recent measurements from the Arctic Stratus Experiment indicate larger droplet concentrations and smaller average droplet radii than the earlier measurements. The larger droplet concentrations and smaller average droplet radii from the Arctic Stratus Experiment are consistent with the large values of CCN reported by Rathore (1983). While it is possible that these differences reflect different efficiencies in measuring small drops, it is also possible that the differences between the observations reflect real differences in aerosol amount and composition. Decreasing (with time) drop sizes and increasing droplet concentrations may be associated with increasing anthropogenic pollution, although natural variations associated with regional and synoptic differences as well as the seasonal phytoplankton productivity cycle may also be factors in variability of this limited sample.

Concentrations of ice forming nuclei in Alaska have been investigated by Hobbs et al. (1971), Isono et al. (1971), and Fountain and Ohtake (1985). Fountain and Ohtake inferred that local nucleus sources play a dominant role in seasonal variations (i.e., wintertime minimum associated with snow-covered ground), while individual episodes of high concentrations were associated with long-range transport, in many instances from Eurasia. From aircraft measurements, Radke et al. (1976) report an average concentration of IFN at -20°C of 0.15 L^{-1}. Jayaweera and Flanegan (1982) investigated the presence of biogenic ice nuclei in the Arctic atmosphere.

Borys (1989) has suggested that the Arctic pollution aerosol may also impact ice nucleation in the Arctic. It has been shown generally and, in the Arctic specifically during springtime (Borys 1983), that polluted air is typically deficient in IFN. This correspondence is believed to be associated with an increased amount of sulfate particles in the polluted air that coagulate with the ice-forming nuclei and effectively deactivate them since sulfate particles act as poor IFN. From observations reported by Curry et al. (1990) during April 1983 and 1986, it seems that significant ice crystal nucleation routinely occurs at temperatures in the range $-15°$ to -20°C. Earlier observations by Witte (1968) described one case with condensate that was predominantly liquid at temperatures as low as -32°C during December 1967, and Jayaweera and Ohtake (1973) found very few ice crystals at temperatures above -20°C during September 1971 and April 1972. Curry et al. (1996) report significant ice nucleation at cloud temperatures as high as -8°C during September 1994. These observations are not inconsistent with the hypothesis that increasing pollution is deactivating IFN, although general conclusions cannot be drawn due to the small number of observations. In any case, the net effect of polluted air on ice nucleation in the Arctic must be regarded as uncertain, as there does not seem to be any simple relationship between sulfate concentration and the temperature at which ice nucleation occurs in the Arctic.

An alternative mechanism for ice nucleation in the Arctic has been proposed. Ohtake (1993) measured the freezing temperature of H_2SO_4 aqueous solutions as a function of concentration in an investigation of the ice nucleation of natural H_2SO_4 mixed aerosols. Ohtake hypothesized that atmospheric ice particles (including the polar diamond dust) may result from the freezing of the sulfate aerosols. The aqueous H_2SO_4 droplets, or aerosols covered with a film of H_2SO_4, can grow larger and become more dilute by absorbing moisture, even at humidities below ice saturation. As H_2SO_4 solution droplets reach a certain dilution, freezing may occur. Diamond dust appearing in the Arctic at temperatures around -22°C corresponds to H_2SO_4 dilutions of about 20% by weight. Once frozen, the crystals will rapidly grow larger under ice-saturated conditions. Blanchet and Girard (1995) have hypothesized that this process can contribute to the dehydration of winter air masses in the Arctic due to fallout of the ice crystals.

In turn, clouds affect aerosols through cloud particle scavenging of aerosols and chemical reactions in clouds that increase the aerosol concentrations. The scavenging of aerosol by clouds and their removal from the atmosphere by precipitation are important sinks for atmospheric aerosol (e.g., Hegg et al. 1984). In-cloud nucleation scavenging occurs by the incorporation of CCN into cloud droplets by activation. Additionally, aerosol particles that do not act as CCN can be incorporated into cloud drops through coagulation processes. As the cloud particles grow to precipitation size, they fall out of the atmosphere and thus act as a sink for atmospheric aerosol. Additionally, precipitation may scavenge aerosol below the cloud base. Snow crystals are approximately twice as efficient as rain drops in scavenging aerosols. Aerosol scavenging processes in polar air mass systems are described by Shaw (1986).

Variations in CCN and IFN have the potential to alter cloud microphysical and optical properties through modifying the cloud particle phase, size, and concentration. Curry et al. (1993) describe the modeled sensitivity of the annual cycle of surface radiation fluxes

over the Arctic Ocean to changes in cloud water droplet effective radius r_e, which might arise in association with changes in aerosol and CCN characteristics (note that a decreasing value of r_e is hypothesized to result from an increase in CCN). An increasing amount of CCN would act to reduce the values of r_e for the liquid water clouds. As drop sizes become smaller, cloud reflectivity increases, reducing the incoming shortwave flux at the surface. Decreasing values of r_e also result in an increase in downward longwave flux. Since the infrared emissivity of Arctic clouds is significantly less than unity (Curry and Herman 1985), decreasing r_e will increase the infrared optical depth and thus the infrared emissivity. It is noted here that the infrared flux of clouds at lower latitudes does not show this sensitivity to r_e since the low-latitude water clouds are typically much more optically thick and emit nearly as blackbodies.

These model results suggest that the first-order "indirect" effects of increasing aerosol concentration in the Arctic will be a slight surface cooling; this cooling is not as pronounced as that expected at lower latitudes because of the sensitivity of the emissivity of Arctic cloud to dropsize variations (due to the low water content of these clouds).

7. Radiation–climate feedback processes

The concepts behind feedback loops have been explained in simple terms by Kellogg (1973). By examining separate feedback loops, one can gain a sense of the direction of the influence of the feedback on a change in the state of the system, whether it is a reinforcing loop or a damping loop, and the relative importance of a given feedback when compared with other feedback loops. The radiation–climate feedback processes that are of interest in the context of the Arctic climate include the snow/ice–albedo feedback, temperature and lapse rate feedbacks, water vapor feedback, and cloud–radiation feedbacks. Radiation–climate feedback processes in the Arctic are important in two different contexts. The first is the context of the impact of the Arctic feedback ppocesses on the energy balance of the planet, and the second is in context of the interactions and feedbacks locally with the underlying surface.

To examine feedback processes locally in the Arctic, we follow the formalism described by Schlesinger (1985) for surface energy balance climate models, whereby the feedback f is defined by

$$f = G_0 \sum_j \frac{\partial N}{\partial I_j} \frac{dI_j}{dT_s}, \tag{1}$$

where N is the downwelling radiative flux, T_s is the surface temperature, and I is the internal dependent variable that gives rise to the feedback. $G_0 = (4\sigma T_s^3)^{-1}$ is the climate system gain in the absence of feedbacks. For an average $T_s = 255$ K, $G_0 = 0.27$. The feedback gain ratio R_f is defined by

$$R_f = \frac{\Delta T_s}{(\Delta T_s)_0} = \frac{1}{1 - f}, \tag{2}$$

where ΔT_s and $(\Delta T_s)_0$ are the changes in parameter T_s in response to an implied forcing with and without the feedback process, respectively. For $f = 0$, $R_f = 1$, representing the zero-feedback temperature change. Because $0 < R_f < 1$ for $f < 0$, the latter represents negative feedback; $R_f > 1$ for $0 < f < 1$ represents a positive feedback. Equations (1) and (2) assume that the feedbacks are linear and independent, which will clearly not hold for large surface flux and temperature perturbations.

a. *Ice–albedo feedback*

The possible importance of high-latitude snow and ice for climate change has been recognized since the 19th century (e.g., Croll 1875). It has been hypothesized that when climate warms, snow and ice cover will decrease, leading to a decrease in surface albedo and an increase in the absorption of solar radiation at the earth's surface, which would favor further warming. The same mechanism works in reverse as climate cools. This climate feedback mechanism is generally referred to as the snow/ice–albedo feedback, which is a positive feedback mechanism. Awareness of this possible ice–albedo feedback has motivated both observational and theoretical studies (e.g., Budyko 1969; Sellers 1969; Robock 1983; Walsh 1983). The ice–albedo feedback has, in fact, proven to be quite important in simulations of global warming in response to increased greenhouse gas concentrations (e.g., Spelman and Manabe 1984; Washington and Meehl 1986; Dickinson et al. 1987; Ingram et al. 1989). The predicted (e.g., IPCC 1990) and observed (e.g., Chapman and Walsh 1993) warming in high latitudes has been at least partly attributed to the ice–albedo feedback mechanism.

The snow/ice–albedo feedback can be separated into the feedbacks associated with land snow/ice and sea ice. Additionally, the land and sea ice albedo feedbacks each may be separated into a feedback associated with the changing horizontal extent of the sea ice and a feedback associated with local processes in the snow or ice pack (e.g., processes related to snow and melt ponds). Different studies have focused on the different components of the snow/ice–albedo feedback. Ingram et al. (1989) summarized the values of the feedback factor δ to range from 0.08 to 0.7 for the snow/ice–albedo feedback mechanism and found that different estimates of the strength of the snow/ice–albedo feedback mechanism made using different models and different experimental designs give substantially different results. It is difficult to compare simulations because some experiments exclude land effects and consider

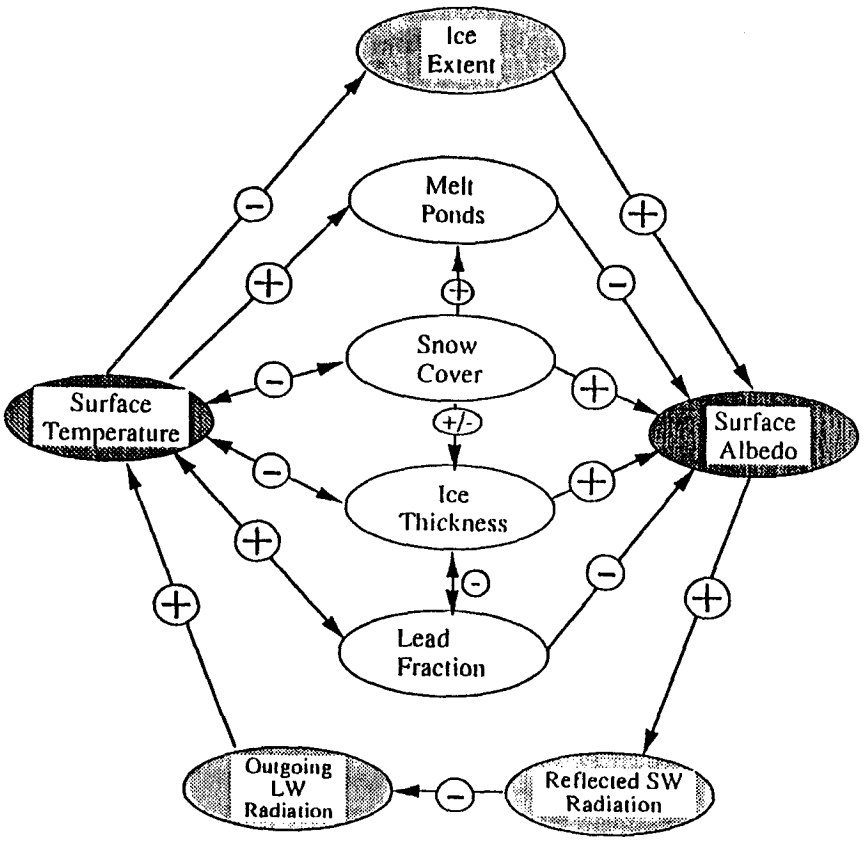

FIG. 11. Schematic diagram of the sea/ice–albedo feedback mechanism. The direction of the arrow indicates the direction of the interaction. A "+" indicates a positive interaction (an increase in the first quantity leads to an increase in the second quantity) and a "−" indicates a negative interaction (an increase in the first quantity leads to a decrease in the second quantity). A "±" indicates either that the sign of the interaction is uncertain or that the sign changes over the annual cycle.

only sea ice and some experiments include cloud changes.

The feedback associated with changes in areal extent of land snow and ice has been described by Cess et al. (1991) and Groisman et al. (1994). Cess et al. (1991) describe an intercomparison of 17 general circulation models, for which perturbations of sea surface temperature were used as a surrogate climate change. Their results indicate that additional amplification or moderation of the snow feedback was caused both by cloud interactions and longwave radiation. One measure of this net effect of snow feedback was found to differ markedly among the 17 climate models, ranging from weak negative feedbacks in some models to strong positive feedback in others. Groisman et al. (1994) observed that Northern Hemispheric snow extent and surface air temperature have varied collinearly over the past 20 years. They propose that the large increase in springtime surface air temperature over the high-latitude land areas of the Northern Hemisphere is associated with snow extent feedback.

Curry et al. (1995a) examined the sea/ice–albedo feedback mechanism associated with local processes occurring within the multiyear ice pack (e.g., processes that influence the duration of the snow cover, ice thickness, lead fraction, ice thickness, and melt pond characteristics). The sea-ice pack albedo feedback mechanism is described as follows (see Fig. 11). A perturbation to the surface energy balance of the sea ice results in a perturbation to surface temperature, melt pond and lead fraction, snow depth, ice thickness, and other sea ice characteristics. Changes in melt pond and lead fraction, snow depth, and sea ice thickness alter the surface albedo, which changes the surface energy balance. Curry et al. (1995a) used a one-dimensional sea ice model to quantify the strength of the ice albedo feedback mechanism and its dependence on sea ice model parameterizations, using (4) with an imposed surface infrared heat flux perturbation and neglecting any other radiation feedback processes. In a comparison of a number of different one-dimensional sea ice models that have the same annually averaged sea ice

thickness for present-day surface forcing, it was shown that there is a substantial difference between the models in terms of sensitivity to surface heat flux perturbations and ice albedo feedback. The magnitude of the positive ice albedo feedback was increased by the inclusion of melt ponds and diminished by the inclusion of ice thickness distribution and ridging. Using these calculations, a value of $R_f = 1.45$ and $f = 0.31$ are determined.

Because of the various crude modeling assumptions used to date and the typical lack of separation of snow–ice albedo feedback from other radiation feedback processes in evaluation of the snow/ice–albedo feedback, the importance of the snow/ice–albedo feedback in the real climate system is still open to question.

b. *Water vapor feedback*

Water vapor feedback is a well-known positive feedback (e.g., Manabe and Wetherald 1967), which is presumed to arise from increased evaporation from warmer oceans. It has frequently been assumed that atmospheric relative humidity would remain approximately constant in a perturbed climate. However, Zhang et al. (1994) have pointed out the dependence of vertical distribution of humidity in a perturbed climate on the convective parameterization. Globally, it was shown that there was a tendency for maximum moisture change at lower levels.

The physical mechanisms associated with water vapor feedback in the Arctic are not necessarily the same as for the rest of the globe because of the relative lack of convective coupling between the surface and the atmosphere and the different thermodynamic and radiative environment. In particular, the effect of water vapor on the net flux of radiation is complicated by the presence of low temperature, low amounts of water vapor and condensed water, and the presence of temperature inversions. The Arctic atmosphere shows a complex vertical structure, associated particularly with inversions of temperature and humidity in the lower troposphere. A low-level humidity inversion is common throughout the year, which arises from the advection of relatively warm moist air over the cold underlying surface. During the cold half of the year, the radiative cooling of the lower troposphere results in the formation of low-level clouds that are crystalline at temperatures below −15°C. Subsequent fallout of these ice crystals dehydrates the lower atmosphere, constraining the relative humidity not to exceed the ice saturation value (Curry 1983). Blanchet and Girard (1995) have hypothesized that the presence of sulfate aerosols may speed the dehydration process during the cold half of the year.

Curry et al. (1995b) investigated the water vapor feedback over the Arctic Ocean, using 10 years of radiosonde data obtained from the Russian drifting stations, by taking advantage of the natural variability associated with the annual cycle and the interannual variability. The basic conclusions drawn from this study were:

(i) A simple relationship between surface temperature and precipitable water over the Arctic Ocean does not exist because of the relative lack of convective coupling between the surface and the atmosphere.

(ii) During the cold half of the year, the dominance of the relative humidity by ice saturation suggests that the relative humidity (with respect to liquid water) will actually *increase* in the lower atmosphere with an increase in temperature, although the length of the period over which ice saturation dominates may be decreased if atmospheric temperatures are uniformly increased over the annual cycle.

(iii) A decrease of relative humidity with increasing temperature occurs in the upper troposphere during summertime, arising from the warmest months in the upper troposphere where there is advection of relatively dry air from the continents rather than from a maritime source.

(iv) Values of the water vapor feedback in the Arctic obtained from examining interannual variability exceed the value obtained from assuming constant relative humidity for a vertically constant temperature increase because of the wintertime constraint of the relative humidity to be near ice saturation, advection of maritime versus continental air masses into the Arctic Basin, and vertical variations in relative humidity changes.

Using the analysis provided by Curry et al. (1995a), values of $R_f = 1.37$ and $f = 0.27$ are determined for the water vapor feedback.

At low latitudes, the lapse-rate temperature feedback is largely compensated by the water vapor feedback, the compensation arising largely through convective processes. In the Arctic, the coupling between the lapse rate and water vapor feedbacks is more complex, especially in the lower atmosphere, and adequate modeling of these feedbacks requires correct simulation of the complex Arctic boundary-layer clouds and their influence on the vertical temperature and humidity profiles.

c. *Cloud–radiation feedback*

Four cloud–radiation feedback mechanisms have been proposed:

1) Wetherald and Manabe (1980) among many others have suggested that changes in cloud fraction and vertical distribution would accompany global warming and further modify surface temperature, although the magnitude and sign of this feedback remains uncertain. Recent 2 $\times$ CO_2 simulations (Wetherald and Manabe 1986; Wilson and Mitchell 1987) show a general decrease in midlevel clouds, increased high-level cloud at all latitudes, and some increases in low clouds at high latitudes, with cloud cover overall reduced in low and midlatitudes. A

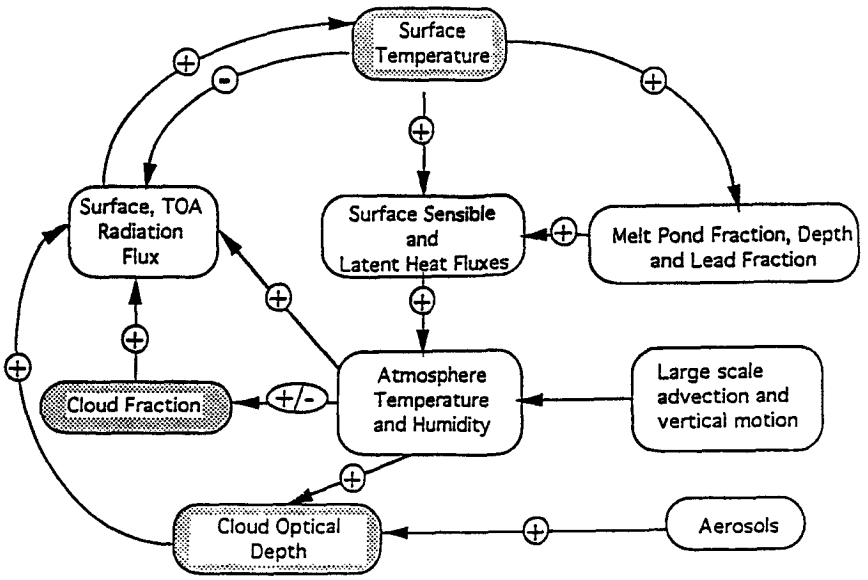

FIG. 12. As in Fig. 11 except for the cloud–radiation feedback mechanism.

summary of 19 atmospheric general circulation models given by Cess et al. (1990) show global cloud feedback ranging from a modest negative value to a strong positive value.

2) Somerville and Remer (1984) have suggested that a negative feedback associated with increasing cloud liquid water content as atmospheric temperature increases would reduce the global surface warming (negative feedback), although Tselioudis and Rossow (1994) show that high-level cloud water content does not exhibit a consistent, simple variation with temperature. Platt and Harshvardhan (1988) have extended these arguments to include ice clouds and showed that the sign of the feedback for the ice clouds depends on the optical depth of the ice clouds and the temperature difference between the ice clouds and the surface.

3) Charlson et al. (1987) have suggested that increased warming would enhance CCN production and change cloud microphysical properties and increase cloud optical depth, thus partially offsetting the global greenhouse warming (negative feedback globally). The increase in pollution aerosol that is expected to parallel increased CO_2 has been hypothesized by Twomey (1977) and Charlson et al. (1992) to have a similar effect. Taylor and Ghan (1992) suggest an increase in cloud drop size with increasing water content.

4) Mitchell et al. (1989) have suggested that, as warming increases, ice cloud that is rapidly depleted by precipitation is replaced by water cloud that is depleted more slowly so that cloud cover increases and cools the surface (negative feedback globally).

Because of the different thermodynamic and radiative environment in the Arctic, conclusions drawn for the globe regarding these cloud feedback processes may be inappropriate over the Arctic Ocean. The cloud–radiation feedback mechanism in the Arctic may be described as follows (see Fig. 12). A perturbation to the Arctic radiation balance may arise from increased greenhouse gas concentrations and/or increasing amounts of aerosol. A perturbation in the surface radiation balance of the snow/ice results in a change in snow/ice characteristics (i.e., ice thickness and areal distribution, surface temperature, and surface albedo). These changes in surface characteristics, particularly the surface temperature and fraction of open water, will modify fluxes of radiation and surface sensible and latent heat, which will modify the atmospheric temperature, humidity, and dynamics. Modifications to the atmospheric thermodynamic and dynamic structure will modify cloud properties (e.g., cloud fraction, cloud optical depth), which will in turn modify the radiative fluxes. An understanding and correct simulation of the cloud–radiation feedback mechanism requires understanding of changes in cloud fractional coverage and vertical distribution as the vertical temperature and humidity profiles change and changes in cloud water content, phase, and particle size as atmospheric temperature and composition changes.

To examine the local feedbacks between Arctic clouds and the surface temperature, we consider the following feedbacks:

$$f = G_0\left[\frac{\partial N}{\partial A_c}\frac{dA_c}{dT_s} + \frac{\partial N}{\partial q_w}\frac{dq_w}{dT_s} + \frac{\partial N}{\partial r_e}\frac{dr_e}{dT_s} + \frac{\partial N}{\partial T_c}\frac{dT_c}{dT_s}\right], \tag{3}$$

where N is the downwelling radiation flux at the surface, A_c is the cloud fraction, q_w is condensed water

content, r_e is the droplet effective radius, T_c is the cloud temperature, and T_s is the surface temperature. The four terms on the right-hand side of (3) represent, respectively, the cloud fraction feedback, the cloud liquid water content feedback, the cloud drop size feedback, and the cloud temperature feedback.

In addition to the modeling studies by Curry and Ebert (1992) and Curry et al. (1993), Kergomard et al. (1993) and Schweiger and Key (1994) have examined the sensitivity of surface fluxes to variations in Arctic cloud characteristics. Using the calculations of Curry et al. (1993) for relatively small perturbations from present-day values, values of $\partial N/\partial A_c$, $\partial N/\partial q_w$, $\partial N/\partial r_e$, and $\partial N/\partial T_c$ are shown in Table 1. Because of uncertainties in evaluating dA_c/dT_s, dq_w/dT_s, dr_e/dT_s, and dT_c/dT_s, there is thus an uncertainty in the sign and magnitude of the components of the cloud–radiation feedback in the Arctic. The discussion below describes the sources of these uncertainties in more detail and attempts to determine a quantitative estimate of the components of the cloud–radiation feedback in the Arctic.

TABLE 1. Evaluation of cloud feedback parameters, f (units for N are W m^{-2}).

Process	$\partial N/\partial I_j$	$\partial I_j/\partial T_s$	f_j	R_f
(Low) cloud fraction ($I = A_c$)	23.93	0.01	0.06	1.06
Cloud water content ($I = q_w$; g kg^{-1})	164.61	0.0072	0.32	1.47
Cloud drop size ($I = r_e$; μm)	−1.77	0	0	1
(Low) cloud temperature ($I = T_c$; K)	2.68	0.8	0.58	2.38

1) CLOUD DISTRIBUTION FEEDBACK

The cloud-distribution feedback mechanism arises from the changes in cloud fraction and vertical distribution that would accompany global warming and further modify surface temperature. How Arctic cloud distribution would change in a changing climate is uncertain. For a perpetual July simulation for a scenario of increasing sea surface temperature by 2°C, LeTreut and Li (1991) found a decrease in Arctic cloud cover up to a level of 300 mb, above which level the cloud fraction increased. Recent 2 × CO_2 simulations (Wetherald and Manabe 1986; Wilson and Mitchell 1987) show an increase in low-level clouds, a decrease midlevel clouds, and an increase in high-level clouds at Arctic latitudes. Clearly, no simple relationship exists between a change in cloud fraction (and vertical distribution) and a change in temperature. In fact, there is probably no unique relationship between a change in temperature and cloud fraction; it is likely to be dependent on the mechanism that results in the temperature increase.

Using the model results from Wetherald and Manabe (1986) and Wilson and Mitchell (1987), we estimate that low cloud fraction increases by 10% for a 10°C increase in surface temperature, for a value of $dA_c/dT_s = 0.01°C^{-1}$ (see Table 1). A positive value of $\partial N/\partial A_c$ along with a positive value of dA_c/dT_s (see Table 1) results in a positive cloud distribution feedback for the Arctic of $f = 0.31$. However, given the difficulties that climate models have in simulating Arctic cloudiness (section 8), the magnitude and even the sign of dA_c/dT_s must be regarded as uncertain.

As atmospheric temperature changes, the fractional cloud cover may change due to changes in atmospheric stability, wind speeds, and advective transports from lower latitudes. Whether fractional cloud cover in the Arctic will increase or decrease in a warming environment is not known with any certainty.

2) CLOUD WATER CONTENT FEEDBACK

Curry et al. (1993) examined the influences of changes in Arctic cloud water content on the surface radiation fluxes and found that an increase in cloud optical depth associated with an increase in atmospheric temperature results in an increase in the annually averaged net downwelling radiation flux at the surface, with the increase in surface flux being most pronounced from June through September.

The cloud water content feedback arises from the assumption that the cloud water content increases with increasing atmospheric temperature if adiabatic processes dominate (e.g., Sommerville and Remer 1984; Platt and Harshvardhan 1988); however, the water content might decrease if nonadiabatic processes dominate (e.g., Tselioudis et al. 1992). Recent observations of cloud liquid water path made by passive satellite microwave radiometry (Curry et al. 1990b) indicate that there is no simple relationship between cloud liquid water path and temperature, and it was suggested that cloud-scale and large-scale dynamics may play a more important role by determining cloud depth and entrainment processes. Tseloudis et al. (1993) reached a similar conclusion with regard to cirrus clouds. Taken together, the observed behavior of colder low-level clouds (Somerville and Remer 1984; Tselioudis et al. 1992) and higher latitude cirrus clouds (Platt and Harshvardhan 1988; Tselioudis and Rossow 1994) suggest that optical thicknesses might increase during a warming trend or that there is a positive feedback between the water content of polar clouds and atmospheric temperature ($dq_w/dT_s > 0$). At subarctic latitudes where solar radiation plays more of a role in the energy balance, such a change would imply a negative cloud–radiative feedback in the annual average but a positive feedback in winter (Tselioudis et al. 1993). In the central Arctic, where LW fluxes play the dominant role, such a change in cloud water content would produce a positive feedback on surface temperatures, but a negative feedback on atmospheric temperatures.

The adiabatic value of dq_w/dT_s for the central Arctic can be estimated from the cloud water content parameterizations used by Curry and Ebert (1992). Cloud liquid water path is parameterized to be a fraction of the adiabatic liquid water path and thus an implicit function of temperature. Ice water content is parameterized to be an explicit function of temperature using the data of Heymsfield and Platt (1984), with separate relationships for upper-level ice crystal clouds and the low-level ice crystal clouds that occur during the cold portion of the year. Other temperature dependencies of the cloud water path include: 1) the variation of the depth of the low-level ice crystal precipitation with temperature so that deeper ice crystal layers are found during winter and 2) the temperature dependence of the phase transition between liquid and ice clouds, which is specified to occur linearly between temperatures $-15°$ to $-22°$C, with clouds having temperatures lower than $-22°$C being completely crystalline. Averaged over the annual cycle, a value of $dq_w/dT_s = 0.0072°\text{C}^{-1}$ (see Table 1) is obtained. A positive value of $\partial N/\partial q_w$ along with a positive value of dq_w/dT_s (see Table 1) results in a positive cloud water feedback for the Arctic of $f = 0.46$. We note here that the cloud phase feedback has been implicitly included here since the temperature of the phase transition has remained constant in these calculations.

The principal uncertainty here is in dq_w/dT_s since it is unclear whether the dynamic controls on cloud water content related to cloud depth and cloud height will dominate the thermodynamic influence on cloud water content feedback. Additionally, this calculation has implicitly assumed that the atmospheric temperature change occurs in response to a surface temperature change and the corresponding convective coupling between the surface in the atmosphere results in an increase in atmospheric water content. The atmospheric warming associated with atmospheric aerosols may not result in a corresponding increase in atmospheric moisture and condensed water; in fact, the opposite is the more likely situation as the atmosphere is stabilized by the warming initially occurring in the atmosphere rather than at the surface.

3) CLOUD DROP SIZE FEEDBACK

Curry et al. (1993) examined the impact of a change in r_e for liquid water clouds on the surface radiative fluxes. Smaller drops resulted in decreased shortwave radiation received at the surface and larger drops resulted in an increased surface shortwave flux. Longwave fluxes showed the reverse, with the smaller drops resulting in a larger surface longwave flux. Examining the annual cycle of the perturbed fluxes showed the surprising result that during summertime, the net surface downward radiation flux decreased both for an increase and decrease in r_e. This nonlinearity arose from the shortwave effects dominating for low values of r_e, while the longwave effects dominated at higher values of r_e. Averaged over the annual cycle, the value of $\partial N/\partial r_e = 1.77\ \text{W m}^{-2}\ \mu\text{m}^{-1}$ (Table 1).

Determination of the cloud drop size feedback requires evaluation of dr_e/dT_s. There are three separate processes that might contribute to dr_e/dT_s in the Arctic: (i) the increase of CCN associated with an increase in oceanic biological productivity in a warmer climate; (ii) an increase in air pollution that parallels an increase in CO_2; and (iii) a change in drop size associated with a change in cloud water content.

The possibility of a feedback between warming ocean temperatures and aerosol concentration was first raised by Shaw (1987) and Charlson et al. (1987). A principal source of sulfate particles and CCN appears to be the oxidation of dimethylsulfide (DMS), which is emitted by phytoplankton in seawater. Therefore, DMS from the oceans may determine the concentrations and size spectra of cloud droplets. If it is assumed that the DMS emissions increase with increasing ocean temperature, there would be an increase in atmospheric aerosol particles. However, the increase of DMS emissions with increasing ocean temperature is not certain. In the Arctic Ocean, the flux of DMS from the ocean occurs through leads, or "cracks" in the sea ice. It seems unlikely that there will be a substantial DMS feedback in the Arctic Ocean associated with a warming: any warming in the Arctic Ocean will first be manifested as a melting of sea ice and will not substantially raise the temperature of the water in the upper ocean. Additionally, the factors that most enhance biological productivity in the Arctic Ocean are sunlight and nutrients; incoming sunlight would be depleted by additional aerosols. In summary, it seems doubtful that there is any temperature–DMS feedback in the Arctic Ocean; an aerosol–sunlight–DMS feedback would be negative. It is anticipated that dr_e/dT_s associated with the local production of DMS in the Arctic is likely to be very small. There may be, however, a component $dr_e/dT_s < 0$ associated with advection of DMS from lower latitudes.

The increase in pollution aerosol, which is expected to parallel increased CO_2, has been hypothesized by Twomey (1977) and Charlson et al. (1992) to have a similar effect on r_e. A direct link between r_e and T_s associated with air pollution has not been quantified; however, an increase in air pollution associated with increasing CO_2 would give $dr_e/dT_s < 0$.

An additional factor that may act to modify r_e is an increase of r_e with an increase in liquid water content (e.g., Stephens 1978; Taylor and Ghan 1992). As liquid water increases, the drop size will increase if the droplet number concentration remains the same, giving rise to $dr_e/dT_s > 0$ if $dq_w/dT_s > 0$. Examination of the data for summertime Arctic stratus (Curry 1986) suggests that the bulk liquid water content is correlated with the droplet concentration rather than the drop size, suggesting that locally the drop size may not increase

with an increase in liquid water content. Heymsfield and Platt (1984) indicate an increase in ice crystal size with atmospheric temperature.

In summary, it is not clear which if any of the cloud drop size feedback mechanisms are important in the Arctic. Since there are both positive and negative drop size feedback mechanisms, it is possible that there is a cancellation among the different effects, and we hypothesize an essentially zero net cloud drop size feedback in the Arctic (Table 1).

d. *Cloud–temperature feedback*

As the atmosphere warms, there will be a feedback associated with increased infrared emission from clouds. Using the radiative transfer model described by Curry and Ebert (1992), we have determined the value of $\partial N/\partial T_c = 2.68$ W m^{-2} °C^{-1} (Table 1). Using the Russian ice island sounding data and surface observations, a value of $dT_c/dT_s = 0.8$ was determined, yielding a value of $f = 0.58$. We note here that cloud altitude feedback has not been included, whereby a change in cloud altitude would alter the cloud temperature.

e. *Cloud phase and precipitation feedbacks*

Curry (1995) has summarized how cloud–aerosol interactions can influence cloud phase. An increased amount of pollution aerosol in the Arctic would increase the amount of cloud water by decreasing the production of precipitation in clouds and thus extending the cloud lifetime (Albrecht 1989). An extended cloud lifetime results in an increase in CCN production by gas-to-particle conversion processes that occur in the presence of liquid water drops. At the same time, an increase in air pollution may result in the effective deactivation of IFN, resulting in a decrease in ice water content and an associated decrease in the amount of ice crystal scavenging of the aerosol and a relative increase in the amount of liquid water content. Thus, there is a positive feedback loop between aerosols and clouds, whereby the larger the aerosol concentration results in increased cloud water content, which increases the cloud production of aerosols and decreases the cloud scavenging of aerosols, resulting in a net increase in cloud aerosols beyond the original input. This hypothesis hinges on a relative decrease of IFN in polluted air; if IFN were increased, then there would be a relative increase of ice water with respect to liquid water, reduced in-cloud production, and increased cloud scavenging of aerosol.

Blanchet and Girard (1995) have hypothesized that the increase of acid to insoluble mass ratio in the Arctic haze would alter the efficiency of forming ice particles and would affect the precipitation rate during the formation of continental polar air masses. An increase in the precipitation flux reduces the atmospheric water content and strength of the atmospheric radiation at the surface. Since enhanced cooling promotes condensation, a feedback is set up between condensation and the greenhouse effect, leading to an accelerated dehydration and cooling cycle during the Arctic winter. This feedback is identified as an indirect effect of aerosols since it alters the radiation balance by changing the microphysics properties of precipitation. This feedback mechanism can explain in part the observed (Kahl et al. 1993) significant surface cooling and strengthening of the temperature inversion trend over the Arctic Ocean during the cold season.

f. *Integration*

The magnitude and even the sign of some of the feedback processes are associated with significant uncertainties. The major uncertainty is associated with the cloud–radiation feedbacks and how cloud characteristics will be altered in a changing climate. The largest uncertainty in assessing the cloud–climate feedback mechanism is the change in cloud cover in response to a change in atmospheric temperature, and thus the sign of the cloud–climate feedback over the Arctic is unknown. Because of the impact of clouds on the surface radiation flux and thus the state of the sea ice surface, the cloud–radiation feedback processes in the Arctic are inextricably linked with albedo feedback processes. Ingram et al. (1989) found that cloud-ice feedbacks were very important; the clouds obscure surface albedo exchanges, thus minimizing their effects. The positive sea ice feedback was quite strong in their model, but they noted that this conclusion is weakened by major uncertainties in the parameterization of Arctic clouds.

If the feedbacks of the individual mechanisms were all mutually independent, the total feedback would be equal to the sum of the individual feedbacks, and the contribution of each mechanism to the total feedback could be individually determined and ranked. Until our physical understanding of the component processes is improved, the interdependence among these processes remains uncertain and unquantified.

Our best estimate at present is that all of the individual climate feedbacks in the Arctic are positive, with the exception of the aerosol–dehydration feedback proposed by Blanchet and Girard (1995). It remains a major task in climate modeling to explain the relative stability of the Arctic climate in the presence of these positive feedbacks. Possibilities include unforeseen negative cloud feedbacks or negative feedbacks between the sea ice and ocean.

8. Climate modeling results

Simulation of the present-day Arctic climate is a prerequisite to modeling perturbed Arctic climates. The database for producing daily gridded analyses over the Arctic Ocean of basic atmospheric dynamic and thermodynamic quantities has been enhanced by the sur-

face pressure and temperature data obtained from drifting sea ice surface buoys (Thorndike et al. 1983) and satellite-derived atmospheric temperature retrievals (e.g., Claud et al. 1991). Improved methods of four-dimensional data assimilation and initialization, such as those employed by the European Centre for Medium-Range Weather Forecasts in their routine initialized analyses, have provided a plausible dataset for diagnostic and climatological studies of Arctic circulation features. However, because of numerical weather prediction model deficiencies in high latitudes, these analyses must be used with caution, particularly with regards to the moisture field. Initialization of numerical weather prediction products and general circulation model climatology is hampered by a relative lack of input data in the Arctic, and the analyzed fields are heavily dependent on the model. There are numerous numerical problems with GCMs at the poles that contribute to the unreliability of their polar climates. Grid-point models typically use filters near the poles to avoid computational instability (e.g., Arakawa and Lamb 1979); these filters can have undesirable effects on model results. Spectral models have serious problems with moisture advection, which become particularly severe near the poles and can lead to spurious negative water vapor amounts (e.g., Williamson and Rasch 1994). The "hole filling" schemes used to address this problem have the effect of diffusing moisture poleward, and this diffusive transport is unphysical. For these reasons, the simulation of moisture advection into the polar regions is particularly challenging for GCMs, casting doubt on their ability to simulate Arctic summer stratus, which is believed to be forced by such moisture advection. All GCMs (including spectral models) do their physics on equal-angle map projections, not equal-area maps. Hence, the grid cell size becomes very small at the poles, which casts doubts on the validity of the subgrid physics parameterizations.

a. Evaluation of 3D climate models at Arctic latitudes

There has been limited examination of the high-latitude performance of atmospheric general circulation models (GCM) (e.g., Herman and Johnson 1980; WCRP 1992; Walsh and Crane 1992; Bromwich et al. 1995). While the present focus is on clouds and radiation, model discrepancies associated with clouds and radiation cannot be interpreted outside of the context of atmospheric dynamics, which are primary determinants of the atmospheric temperature, humidity, and cloud characteristics.

In the first study of the performance of a GCM in the Arctic, Herman and Johnson (1980) found that the Goddard Laboratory for the Atmospheric Sciences (GLAS) GCM determined the following deficiencies: the wintertime Siberian anticyclone is seriously underestimated, unrealistically strong sea level pressure gradients exist in the Beaufort Sea during summer, wintertime surface temperatures are in general too warm in the Arctic with biases as large as 9°C in the central Arctic, and the model significantly underpredicts the summertime cloud cover and overpredicts the wintertime cloud cover.

Walsh and Crane (1992) noted large variations among polar climates as simulated by different GCMs. In a comparison of Arctic climatologies generated by five different climate models, biases of up to 5°–10°C in surface temperatures relative to observations were apparent over much of the Arctic. The simulated sea level pressure pattern varied widely from model to model, in some cases showing the absence of the Beaufort Sea anticyclone.

The performance of GCMs in high latitudes in the context of clouds, radiation, and the surface energy balance is reported by WCRP (1992). In an intercomparison of 14 GCMs, Boer (1992) found that: all models display anomalously low temperatures in the upper troposphere, many models simulate near surface temperatures that are too low while other simulations are too high, all models predict too much precipitation in the Arctic, and there are large variations among models in the net surface heat flux. Cattle (1992) examined the cloud climatology and surface insolation in the Arctic produced by the UKMO GCM and found that summertime cloud amount determined using an interactive cloud scheme is too high during summer, resulting in summertime surface insolation that is only half of the observed values. Klinker (1992) compared the modeled TOA fluxes with those determined from ERBE and found agreement to within 10 W m^{-2} during winter; however, during July the net model TOA radiation was larger than the ERBE observations by nearly 10 W m^{-2}; surface insolation was determined to be far too large during the Arctic summer.

To promote more systematic evaluations and comparisons of GCMs, the Atmospheric Model Intercomparison Project (AMIP) was organized in 1990 (Gates 1992). Approximately 30 GCMs have completed a ten-year (1979–88) simulation using observed monthly averaged values of sea surface temperature and sea ice extent. The AMIP results have been analyzed for the Arctic by Tao et al. (1995), Chen et al. (1995), Bromwich et al. (1994), and Khattsov et al. (1995). Tao et al. (1995) examined Arctic surface air temperatures for 19 different models and found zonally and seasonally averaged temperatures to have a range of 8°C during summer and 17°C during winter near the pole. Cloud coverage modeled by 5 GCMs and analyzed by Chen et al. (1995) showed that discrepancies in longitudinally and annually averaged modeled cloud cover are as large as 60% in the Arctic. Modeled mean wintertime cloud cover varied from 2% to 75% and summertime cloud cover varied from 5% to 95%. Walsh et al. (1995) examined the longitudinally and annually averaged cloud coverage for 19 models and found values

ranging from 40% to 90%. Khattsov et al. (1995; unpublished manuscript) showed June surface insolation values to range from 85 to 185 W m^{-2} (compared with 310 W m^{-2} observed).

Detailed analyses of the Arctic climatology of the NCAR Community Climate Model (CCM) have been described by Battisti et al. (1992) and Tzeng and Bromwich (1994). Battisti et al. (1992) found that Version 1 (CCM1) demonstrated that the TOA incoming solar radiation and outgoing longwave radiation are too large in the model because of the errors in the simulated temperature and cloudiness for this area. Over the Arctic basin, the CCM1 simulates large amounts of low clouds in winter and almost none in summer (opposite to what is observed), arising from errors in simulating the large-scale atmospheric dynamics. Version 2 (CCM2) was designed to remedy most of the shortcomings of CCM1. Battisti et al. (1992) then found that the Beaufort Sea wintertime anticyclone is not simulated by CCM2. Improvements to the boundary-layer parameterization resulted in an improvement to the simulation of the summertime cloud fraction to 50% total cloud cover, although this is still significantly lower than the observed cloud fraction.

Randall et al. (1985) cite a substantial underestimate of the summertime Arctic Ocean cloud cover by the CSU GCM. Lappen (1995) has conducted a detailed analysis of the Arctic cloud and radiation climate as simulated by the CSU GCM and comparison with observations. The following problems were identified in the modeled meteorological parameters, relative to observations:

1) The temperatures over the entire Arctic in July are too warm. The January temperatures agree with observations except for in the Kara and Barents Sea region where they are too cold.
2) Boundary-layer wind speeds appear to be too strong, independent of month and location.
3) Wind directions agree well with the observations except for the Bering Strait in January, the Norwegian Sea in July, and the Alaska Peninsula in January.
4) Mean sea level pressure is low by 10–20 mb across the Arctic universally in January, although the relative changes in pressure are captured.
5) The GCM overpredicts geopotential height in July by 100 m universally.

These errors in meteorological parameters gave rise to the following errors in clouds and radiation:

1) Low and clouds are severely underpredicted over the Arctic Ocean in July and overpredicted in January.
2) The GCM tends to overpredict high clouds with exception of underprediction in the eastern Arctic Ocean.
3) The summertime net surface shortwave radiation flux over the Arctic Ocean shows good agreement with observations due to compensating errors associated with a high surface albedo and underprediction of clouds.
4) The surface net longwave radiation over the Arctic Ocean is too high during January and close to observed values during July due to a combination of low surface temperatures and values of the downwelling longwave radiation that are too low.
5) TOA shortwave and longwave cloud forcing are both too weak during July, yielding a net value that is close to the observed.

One of the critical difficulties in accurately simulating the cloud and radiation climate of the Arctic is that cloud formation depends on large-scale atmospheric dynamics. Errors in the Arctic large-scale dynamics can arise from problems arising at lower latitudes (e.g., Tzeng and Bromwich 1994). Additionally, significant errors in the Arctic were shown by Tzeng and Bromwich (1994) to be associated with low model resolution. Physical parameterizations in GCMs related to clouds and radiation are incapable of capturing key features of the Arctic climate. Toward addressing these deficiencies in Arctic climate simulations, the Arctic Region Climate System Model (ARCSyM) has been developed (Walsh et al. 1993; Lynch et al. 1995). The ARCSyM is based upon the NCAR regional climate model (Giorgi et al. 1993a,b), but special attention has been paid to the inclusion of the ice phase in the atmosphere and the ocean and on land. Lynch et al. (1995) have performed winter and summer simulations of the Alaskan Arctic climate. The model climatology shows general spatial patterns consistent with observations, although biases appeared because of the relatively low evaporation rates resulting from interactions between the cloud–radiation scheme and surface processes, particularly over land. The inclusion of sea ice dynamics was shown to have a substantial impact on model results for winter. The model was shown to be sensitive to details of the cloud microphysical parameterization.

b. Modeling perturbations to the Arctic climate

Since the GCM simulation of the present-day Arctic climate shows serious deficiencies, simulations of perturbed climate regimes must be seriously questioned, and their use for predictive purposes should be interpreted with caution. Nevertheless, simulations of perturbed climate states can provide important insights into modeling the climate system.

Climate model experiments with doubled CO_2 concentrations have found that the warming is amplified in the Arctic due to the retreat of the Arctic Ocean sea ice (e.g., Houghton et al. 1990; Schlesinger and Jiang 1991). Local Arctic temperature increases as large as 20°C during wintertime have been simulated by Wetherald and Manabe (1986) in a doubling CO_2 experiment. Substantial differences exist between predictions

made by different models of the high-latitude amplification of CO_2 warming (e.g., Schlesinger and Jiang 1991).

Manabe et al. (1991) compared the results from a coupled global ocean–atmosphere model for an equilibrium response versus a transient response to CO_2 doubling. In the transient simulation, the atmospheric carbon dioxide concentration is increased by 1% per year (compounded). In the transient simulation, most of the Arctic temperature change occurs more than 65 years after the beginning of the CO_2 increase. After 70 years of integration in the transient experiment (corresponding to a CO_2 doubling), the Arctic Ocean surface warming is about 30% less than the warming simulation as an equilibrium response to a doubling of CO_2.

Fletcher et al. (1973), Warshaw and Rapp (1973), and Royer et al. (1990) performed extreme sensitivity tests with GCMs, arbitrarily removing the Arctic sea ice. Royer et al. found that removal of the Arctic sea ice led to a reduction in the Arctic cloud cover. This is intriguing because a reduction in cloud cover favors more solar warming of the ocean, thus tending to prevent the return of the sea ice.

Graf (1992) used a GCM to simulate the response of the global climate to a large increase in Arctic stratospheric aerosol associated with a high-latitude volcanic eruption. The results of this experiment suggest that the radiation deficit associated with the volcanic aerosol is a possible external forcing factor for severe climatic anomalies not only in the area directly affected by the reduced radiation, but also in the Tropics. Enhanced snow cover in regions of Asia was simulated and was associated with prolonged winter monsoon conditions, a weak Asian summer monsoon, and a weakened Walker circulation.

Blanchet (1989, 1990) examined the impact of incorporating the radiative effects of moist Arctic aerosols associated with the Arctic Haze pollution aerosol (impact of aerosols on cloud properties was not included) into a general circulation climate model. From these simulations, it was found that the net radiative effects of the moist aerosols was in part balanced by a reduction in the meridional transport of heat, and consequently, the result was a marginal increase in the lower-tropospheric temperatures in the Arctic.

9. Conclusions

Based on the climate model experiments, it appears that the Arctic and particularly the ice pack should be a sensitive indicator of climate change. Although the current GCMs show wide discrepancies in their simulations of present Arctic climate and their ability to predict future climate changes is open to serious question, nearly all GCMs exhibit amplified greenhouse warming in the Arctic, and it is natural to ask whether such warming is being observed. In an examination of the surface temperature and sea ice record, Chapman and Walsh (1993) found that summertime Arctic sea ice extent shows a small significant decrease, with no decrease in ice extent evident in winter. Warming is observed over the high-latitude land areas during winter and spring, with the temperature trends over the sub-Arctic seas being smaller and even negative in the southern Greenland region. Kahl et al. (1993) report no significant trend in Arctic Ocean surface temperature over the past 40 years. Johannessen et al. (1995) argue that satellite passive microwave imagery indicates a significant decrease in Arctic ice extent during the period 1978–1987, followed by a more rapid decrease from 1987 to 1994. Unfortunately, the databases that can be used to assess climate change are very limited in the Arctic, and studies looking for clear greenhouse warming trends are inconclusive. The relative lack of observed warming and relatively small ice retreat may indicate that GCMs are overemphasizing the sensitivity of climate to high-latitude processes. Alternatively, sea ice thickness or volume (which is not routinely observed) may be a more relevant parameter with which to infer climate change.

A key question remains as to the role that clouds and the associated feedbacks play in modulating the greenhouse warming in the Arctic. In this paper we have provided an overview of the current state of knowledge regarding Arctic clouds and radiation. The basic annual cycle of cloud and radiation characteristics remains uncertain enough that the precise role of cloud feedbacks cannot be determined. Although some modeling studies have been conducted of boundary-layer clouds, these models remain largely unvalidated by observations. Climate model simulations of Arctic clouds and radiation disagree with each other and with observations. The full potential of satellite remote sensing of clouds and radiation characteristics of the Arctic is not known. All of these problems arise from a lack of comprehensive observations that can be used to check remote sensing analyses and model parameterizations.

Toward improving the representation of Arctic clouds and radiation in GCMs, better climatological data is needed. Model parameterizations specifically formulated for the Arctic environment are also needed. To achieve this, it will be necessary to collect data not only on the Arctic climatic state itself, but also on the physical processes that produce and maintain that state. In addition, it is important that climate modelers participate in these field studies, contribute to their planning and execution, and make use of the data. Below are listed some of the key scientific issues related to Arctic clouds and radiation that have significant uncertainties at present.

1) What is the spectral distribution of longwave radiation and in particular what is the role of the 20-μm "rotation-band window" region in regulating the surface and atmospheric temperature in the Arctic?

2) What are the effects of springtime "Arctic haze" on the absorption of solar radiation in polar clouds?

3) How do the reflectance and transmittance of the clouds and the surface depend on the high solar zenith angles typical of the Arctic?

4) What is the role of "clear-sky" ice crystal precipitation in determining the longwave radiation fluxes?

5) What are the shortwave radiative effects of the horizontally inhomogeneous stratocumulus clouds over the horizontally inhomogeneous, highly reflecting snow/ice surface?

6) How do the optical properties of the Arctic surface vary in response to changes in snow characteristics (thickness, age, temperature, contamination), thinning of the ice, and melt pond formation?

7) What is the influence of leads and other open water on cloud properties when there is a large surface temperature contrast with the ice?

8) How does the extreme static stability and low atmospheric water vapor content of the Arctic lower troposphere, particularly during winter, affect the flow energy across the air–sea interface?

9) What is the mechanism that leads to the spectacular multiple-layering of Arctic Ocean summer cloud systems?

10) How does the transition of low clouds from liquid to crystalline depend on temperature and aerosol characteristics, and how does the springtime transition differ from the autumnal transition?

11) How do clouds and radiation interact with the summertime melting of snow and sea ice?

12) What are the potential feedbacks among cloud–radiation, surface warming, and the release of methane into the atmosphere from the permafrost?

13) How is the cloud–radiation feedback coupled to the ice-albedo feedback?

In response to the above scientific issues, the Atmospheric Radiation Measurement (ARM) program has proposed the North Slope of Alaska and Adjacent Arctic Ocean (NSA/AAO) as a primary measurement site. It is anticipated that measurements will begin in 1997 in the vicinity of Barrow, Alaska.

A coordinated research program has been formulated to address the interactions among the surface energy balance, atmospheric radiation, and clouds over the Arctic Ocean. SHEBA (Surface Heat Budget of the Arctic Ocean) is a component of the U.S. Global Change Research Program and the Arctic Climate System (ACSYS) Study of the World Climate Research Program. Some of the scientific objectives of SHEBA are shared by the National Aeronautics and Space Administration (NASA) FIRE Phase III program and the DOE ARM program. Activities of these three coordinated research programs will culminate in a major field experiment in the Arctic Ocean beginning in September 1997 (Moritz et al. 1993).

Acknowledgments. Support for this research was provided by the Department of Energy Atmospheric Radiation Measurement Program and NSF OPP-9504261 to the University of Colorado and by NASA's Climate Program under Grant NAG-1-893 and by the Office of Naval Research under Contract N00014-89-J-1364, both to Colorado State University. Comments on the manuscript from Professor John Walsh are very much appreciated.

REFERENCES

Albrecht, B. A., 1989: Aerosols, cloud microphysics, and fractional cloudiness. *Science,* **245,** 1227–1230.

Andreas, E. L., 1980: Estimation of heat and mass fluxes over Arctic leads. *Mon. Wea. Rev.,* **108,** 2057–2063.

——, and Coauthors, 1979: The turbulent heat flux from Arctic leads. *Bound.-Layer Meteor.,* **17,** 57–91.

——, M. W. Miles, R. G. Barry, and R. C. Schell, 1990: Lidar-derived particle concentration in plumes from Arctic leads. *Ann. Glaciol.,* **14,** 9–12.

Arakawa, A., and V. R. Lamb, 1979: Energy and potential energy conserving scheme for the shallow-water equations. *Bull. Amer. Meteor. Soc.,* **60,** p. 608.

Baker, M., and J. Latham, 1979: The evolution of droplet spectra and the rate of production of embryonic raindrops in small cumulus clouds. *J. Atmos. Sci.,* **36,** 1612–1615.

Barrie, L. A., 1986: Arctic air pollution: An overview of current knowledge. *Atmos. Environ.,* **19,** 1995–2010.

Battisti, D. S., D. L. Williamson, and R. E. Moritz, 1992: Simulation of the arctic climatology with the NCAR CCM-2. Preprints, *Third Conf. on Polar Meteorology and Oceanography,* Portland, OR, Amer. Meteor. Soc., 133–136.

Belmont, A. D., 1957: Lower tropospheric inversions at Ice Island T-3. *Polar Atmosphere Symposium,* R. Sutcliffe, Ed., Pergamon Press, 341 pp.

Benson, C. S., 1970: Ice fog. *Weather,* **25,** 11–18.

Beryland, T. G., and L. A. Strokina, 1980: *Global Distribution of Total Cloud Amount.* Gidrometeoizdata, Leningrad (translated by S. Warren, University of Washington).

Bigg, E. K., 1980: Comparison of aerosol at four baseline atmospheric monitoring stations. *J. Appl. Meteor.,* **19,** 521–533.

Blanchet, J.-P., 1989: Toward estimation of climatic effects due to arctic aerosols. *Atmos. Environ.,* **23,** 2609–2625.

——, 1990: The effects of arctic aerosols on a general circulation model simulation: A sensitivity study. *Aerosols and Climate,* P. V. Hobbs and M. P. McCormick, Eds., A. Deepack.

——, and R. List, 1987: On radiative effects of anthropogenic aerosol components in Arctic haze and snow. *Tellus,* **39B,** 293–317.

——, and E. Girard, 1995: Water vapour-temperature feedback in the formation of continental arctic air: Implication for climate. *Sci. Total Environ.,* **160/161,** 793–802.

Boer, G. J., 1992: Some aspects of AGCM behaviour in polar regions. WCRP Report on a Workshop on Polar Radiation Fluxes and Sea-Ice Modelling. E. Raschke, H. Cattle, P. Lemke, and W. Rossow, Eds. WMO/TD, 52–57.

Borys, R. D., 1989: Studies of ice nucleation by arctic aerosol on AGASP-II. *J. Atmos. Chem.,* **9,** 169–185.

Bowling, S. A., 1975: The effect of ice fog on thermal stability. *Northern Engineer,* **7,** 32–40.

Bradley, R. S., F. T. Keiming, and H. F. Diaz, 1992: Climatology of surface-based inversions in the North American Arctic. *J. Geophys. Res.,* **97,** 15 699–15 712.

Briegleb, B. P., P. Minnis, V. Ramanathan, and E. F. Harrison, 1986: Comparison of clear-sky albedos inferred from satellite observations and model computations. *J. Climate Appl. Meteor.,* **25,** 214–226.

Broecker, W. S., M. Andreae, W. Wolfli, H. Oescher, G. Bonani, J. Kennett, and D. Peteet, 1988: The chronology of the last deglaciation: Implications to the cause of the Younger Dryas event. *Paleo-Oceanogr.*, **3,** 1–19.

——, J. P. Kennett, and B. P. Flower, 1989: Routing of meltwater from the Laurentide ice sheet during the Younger Dryas cold episode. *Nature,* **318,** 318–321.

Bromwich, D. H., R.-Y. Tzeng, and T. R. Parish, 1994: Simulation of the modern Arctic climate by the NCAR CCM1. *J. Climate,* **7,** 1050–1069.

——, B. Chen, and X. Pan, 1995: Intercomparison of simulated polar climates by global climate models. Preprints, *Fourth Conf. on Polar Meteorology and Oceanography.* Dallas, TX, Amer. Meteor. Soc., (J9)14–(J9)19.

Buckley, R. G., and H. J. Trodahl, 1987: Scattering and absorption of visible light by sea ice. *Nature,* **326,** 865–867.

Budyko, M. I., 1969: The effect of solar radiation variations on the climate of the earth. *Tellus,* **21,** 611–619.

Busch, N., U. Ebel, H. Kraus, and E. Schaller, 1982: The structure of the subpolar inversion capped ABL. *Arch. Meteor. Geophys. Bioklimatol.,* **331,** 1–18.

Byers, C. A., and W. J. Stringer, 1992: Unusual cloud forms in the arctic winter boundary layer. Preprints, *Third Conf. on Polar Meteorology and Oceanography,* Portland, OR, Amer. Meteor. Soc., 7–10.

Cappellaz, J. A., I. Fung, and A. M. Thompson, 1993: The atmospheric CH4 increase since the last glacial maximum. Part I: Source estimates. *Tellus,* **45B,** 228–241.

Catchpole, A., and J. Moodie, 1971: Multiple reflection in arctic regions. *Weather,* **26,** 157–161.

Cattle, H., 1992: Cloud schemes and the simulation of arctic surface insolation and sea ice in the UKMO climate model. WCRP Report on a Workshop on Polar Radiation Fluxes and Sea-Ice Modelling. E. Raschke, H. Cattle, P. Lemke, and W. Rossow, Eds., WMO/TD, 58–61.

Cess, R. D., G. L. Potter, J. P. Blanchet, G. J. Boer, A. D. Del Genio, M. Deque, V. Dymnikov, V. Galin, W. L. Gates, S. J. Ghan, J. T. Kiehl, A. A. Lacis, H. LeTreut, Z.-X. Li, X.-Z. Liang, B. J. McAvaney, V. P. Meleshko, J. F. B. Mitchell, J.-J. Morcrette, D. A. Randall, L. Rikus, E. Roeckner, J. F. Royer, U. Schlese, D. A. Sheinin, A. Slingo, A. P. Sokolov, K. E. Taylor, W. M. Washington, R. T. Wetherald, I. Yagai, and M.-H. Zhang, 1990: Intercomparison and interpretation of climate feedback processes in 19 atmospheric general circulation models. *J. Geophys. Res.,* **95,** 16 601–16 615.

——, ——, M.-H. Zhang, J.-P. Blanchet, S. Chalita, R. Colman, D. A. Dazlich, A. D. DelGenio, V. Dymnikov, V. Galin, D. Jerrett, E. Keup, A. A. Lacis, H. LeTreut, X.-Z. Liang, J.-F. Mahfouf, B. J. McAvaney, V. P. Meleshko, J. F. B. Mitchell, J.-J. Morcrette, P. M. Norris, D. A. Randall, L. Rikus, E. Roeckner, J.-F. Royer, U. Schlese, D. A. Sheinin, J. M. Slingo, A. P. Sokolov, K. E. Taylor, W. M. Washington, R. T. Wetherald, and I. Yagai, 1991: Interpretation of snow–climate feedback as produced by 17 general circulation models. *Science,* **253,** 888–892.

Chapman, W. L., and J. E. Walsh, 1993: Recent variations of sea ice and air temperature in high latitudes. *Bull. Amer. Meteor. Soc.,* **74,** 33–47.

Charlson, R. J., J. E. Lovelock, M. O. Andreae, and S. G. Warren, 1987: Oceanic phytoplankton, atmospheric sulphur, cloud albedo and climate. *Nature,* **326,** 655–661.

——, S. E. Schwartz, J. M. Hales, R. D. Cess, J. A. Coakely Jr., J. E. Hansen, and D. J. Hofmann, 1992: Climate forcing by anthropogenic aerosols. *Science,* **255,** 423–430.

Chen, B., D. H. Bromwich, K. M. Hines, and X. Pan, 1995: Simulations of the 1979–1988 polar climates by global climate models. *Ann. Glaciol.,* **21,** 83.

Choudhury, B. J., and A. T. C. Chang, 1981: The albedo of snow for partially cloudy skies. *Bound.-Layer Meteor.,* **20,** 371–389.

Chylek, P., and J. Coakely, 1973: Man-made aerosol and the heating at atmosphere over polar regions. *Proc. 24th Alaska Science Conf.,* Fairbanks, AK, 159–160.

Clarke, A. D., and K. J. Noone, 1985: Soot in the Arctic snowpack: A cause for perturbations in radiative transfer. *Atmos. Environ.,* **19,** 2045–2053.

Claud, C., N. A. Scott, A. Chedin, and J. C. Gascard, 1991: Assessment of the accuracy of atmospheric temperature profiles retrieved from TOVS observations by the 3I method in the European Arctic: Application for weather analysis. *J. Geophys. Res.,* **96,** 2875–2887.

Cogley, J. G., and A. Henderson-Sellers, 1985: The albedo of ice in general circulation models. Trent Tech. Note 85-2, 39 pp. [Available from Trent University, Peterborough, ON, CANADA.]

Croll, J., 1875: *Climate and Time in Their Geological Relations, a Theory of Secular Change of the Earth's Climate.* Daldy, Isbister.

Curry, J. A., 1983: On the formation of continental polar air. *J. Atmos. Sci.,* **40,** 2279–2292.

——, 1986: Interactions among turbulence, radiation and microphysics in Arctic stratus clouds. *J. Atmos. Sci.,* **43,** 90–106.

——, 1987: Role of radiative cooling in the formation of cold-core anticyclones. *J. Atmos. Sci.,* **44,** 2575–2592.

——, 1995: Interactions among aerosols, clouds and climate of the arctic ocean. *Sci. Total Environ.,* **160/161,** 777–791.

——, and G. F. Herman, 1985: Infrared radiative properties of summertime Arctic stratus clouds. *J. Climate Appl. Meteor.,* **24,** 526–538.

——, and E. E. Ebert, 1990: Sensitivity of the thickness of Arctic sea ice to the optical properties of clouds. *Ann. Glaciol.,* **14,** 43–46.

——, and ——, 1992: Annual cycle of radiation fluxes over the Arctic Ocean: Sensitivity to cloud optical properties. *J. Climate,* **5,** 1267–1280.

——, and L. F. Radke, 1993: Possible role of ice crystals in ozone destruction of the lower Arctic atmosphere. *Atmos. Environ.,* **27A,** 2873–2879.

——, E. E. Ebert, and G. F. Herman, 1988: Mean and turbulent structure on the summertime Arctic cloudy boundary layer. *Quart. J. Roy. Meteor. Soc.,* **114,** 715–746.

——, F. G. Meyer, and E. E. Ebert, 1989a: Cloudless ice crystal precipitation in the polar regions. *IRS'88 Current Problems in Atmospheric Radiation,* J. Lenoble and J. F. Creleyn, Eds., A. Deepak, 80–83.

——, L. F. Radke, C. A. Brock, and E. E. Ebert, 1989b: Arctic ice-crystal haze. *Symp. on the Role of Clouds in Atmospheric Chemistry and Global Climate,* Anaheim, CA, Amer. Meteor. Soc., 114–117.

——, F. G. Meyer, L. F. Radke, C. A. Brock, and E. E. Ebert, 1990a: Occurrence and characteristics of lower tropospheric ice crystal in the Arctic. *Int. J. Climatol.,* **10,** 749–764.

——, C. D. Ardeel, and L. Tian, 1990b: Liquid water content and precipitation characteristics of stratiform clouds as inferred from satellite microwave measurements. *J. Geophys. Res.,* **95,** 16 659–16 671.

——, E. E. Ebert, and J. L. Schramm, 1993: Impact of clouds on the surface radiation balance of the Arctic Ocean. *Meteor. Atmos. Phys.,* **51,** 197–217.

——, J. L. Schramm, and E. E. Ebert, 1995a: On the ice albedo climate feedback mechanism. *J. Climate,* **8,** 240–247.

——, ——, M. C. Serreze, and E. E. Ebert, 1995b: Water vapor feedback over the Arctic Ocean. *J. Geophys. Res.,* **100,** 14 223–14 229.

——, J. O. Pinto, T. Benner, and M. Tschudi, 1996: Evolution of the cloudy boundary layer during the autumnal freezing of the Beaufort Sea. *J. Geophys. Res.,* in press.

Dergach, A. L., G. M. Zabrodsky, and V. G. Morachevsky, 1960: The results of a complex investigation of the type st-sc clouds and fogs in the Arctic. *Bull. Acad. Sci. USSR, Geophys. Ser.,* **1,** 66–70.

Dickinson, R. E., G. A. Meehl, and W. M. Washington, 1987: Ice-albedo feedback in a CO_2-doubling simulation. *Clim. Change,* **10,** 241–248.

Dirmhirn, I., and F. D. Eaton, 1975: Some characteristics of the albedo of snow. *J. Appl. Meteor.,* **14,** 375–379.

Dozier, J., and S. G. Warren, 1982: Effect of viewing angle on the infrared brightness temperature of snow. *Water Resour. Res.,* **18,** 1424–1434.

——, R. E. Davis, A. T. C. Chang, and K. Brown, 1988: The spectral bidirectional reflectance of snow. *Proc., Fourth Int. Colloq. Spectral Signatures of Objects in Remote Sensing,* Eur. Space Agency Spec. Publ., ESA SP-287, 87–92.

Dutton, E. G., R. S. Stone, D. W. Nelson, and B. G. Mendonca, 1991: Recent interannual variations in solar radiation, cloudiness, and surface temperature at the South Pole. *J. Climate,* **4,** 848–858.

Ebert, E. E., 1989: Analysis of polar clouds from satellite imagery using pattern recognition and a statistical cloud analysis scheme. *J. Appl. Meteor.,* **28,** 282–299.

——, and J. A. Curry, 1993: An intermediate one-dimensional thermodynamic sea ice model for investigating ice–atmosphere interactions. *J. Geophys. Res.,* **98,** 10 085–10 109.

Ellingson, R. G., J. A. Curry, K. Stamnes, J. E. Walsh, and B. D. Zak, 1996: Overview of north slope of Alaska/adjacent Arctic Ocean (NSA/AAO) science issues and siting strategies. *J. Climate,* submitted.

Emery, C. A., R. M. Haberle, and T. P. Ackerman, 1992: A one-dimensional modelling study of carbonaceous haze effects on the springtime arctic environment. *J. Geophys. Res.,* **97,** 20 599–20 613.

Ferek, R. J., P. V. Hobbs, and G. F. Cota, 1995: Dimethyl sulfide in the Arctic atmosphere. *J. Geophys. Res.,* **100,** 26 093–26 104.

Fett, R. W., S. D. Burk, W. T. Thompson, and T. L. Kozo, 1994: Environmental phenomena of the Beaufort Sea observed during the Leads Experiment. *Bull. Amer. Meteor. Soc.,* **75,** 2131–2145.

Fletcher, J. O., 1965: The heat budget of the Arctic basin and its relation to climate. The Rand Corporation, R-444-PR, 175 pp.

——, Y. Mintz, A. Arakawa, and T. Fox, 1973: Numerical simulation of the influence of Arctic sea ice on climate. *Energy Fluxes over Polar Surfaces: Proc. IAMAP/IAPSO/SCAR/WMO Sym.,* Moscow, USSR, World Meteorological Organization, 181–218.

Fountain, A. G., and T. Ohtake, 1985: Concentrations and source areas of ice nuclei in the Alaskan atmosphere. *J. Climate Appl. Meteor.,* **24,** 377–382.

Francis, J. A., 1994: Improvements to TOVS retrievals over sea ice and applications to estimating Arctic energy fluxes. *J. Geophys. Res.,* **99**(10), 395–408.

——, T. P. Ackerman, K. B. Katsaros, R. J. Lind, and K. L. Davidson, 1991: A comparison of radiation budgets in the Fram Strait summer marginal ice zone. *J. Climate,* **4,** 218–235.

Gates, W. L., 1992: AMIP: The Atmospheric Model Intercomparison Project. *Bull. Amer. Meteor. Soc.,* **73,** 1962–1970.

Gavrilova, M. K., 1963: Radiation climate of the Arctic. Gidrometeorologichskeo Izd., 178 pp. (English translation by Israel Prog. for Scientific Translation, 1966).

Giorgi, F., M. R. Marinucci, and G. T. Bates, 1993a: Development of a second generation Region Climate Model (RegCM2). Part I: Boundary layer and radiative transfer processes. *Mon. Wea. Rev.,* **121,** 2794–2813.

——, ——, and ——, 1993b: Development of a second generation Region Climate Model (RegCM2). Part II: Convective processes and assimilation of lateral boundary conditions. *Mon. Wea. Rev.,* **121,** 2814–2832.

Gorshkov, S. G., 1983: *World Ocean Atlas.* Vol. 3, *The Arctic Ocean.* Pergamon Press.

Gotaas, Y., and C. S. Benson, 1965: The effect of suspended ice crystals on radiative cooling. *J. Appl. Meteor.,* **4,** 446–453.

Graf, H.-F., 1992: Arctic radiation deficit and climate variability. *Climate Dyn.,* **7,** 19–28.

Grenfell, T. C., 1983: A theoretical model of the optical properties of sea ice in the visible and near infrared. *J. Geophys. Res.,* **88,** 9723–9735.

——, and G. A. Maykut, 1977: The optical properties of ice and snow in the Arctic Basin. *J. Glaciol.,* **18,** 445–463.

——, and D. K. Perovich, 1984: Spectral albedos of sea ice and incident solar irradiance in the southern Beaufort Sea. *J. Geophys. Res.,* **89,** 3573–3580.

Groisman, P. Y., T. R. Karl, and R. W. Knight, 1994: Observed impact of snow cover on the heat balance and the rise of continental spring temperatures. *Science,* **263,** 198.

Hahn, C. J., S. G. Warren, J. London, R. M. Chervin, and R. Jenne, 1984: Atlas of simultaneous occurrence of different cloud types over land. NCAR Tech. Note, TN-241+STR, National Center for Atmospheric Research, Boulder, CO, 21 pp.

——, ——, and ——, 1995: The effect of moonlight on observation of cloud cover at night, and application to cloud climatology. *J. Climate,* **8,** 1429–1446.

Harrison, E. F., P. Minnis, B. R. Barkstrom, V. Ramanathan, R. D. Cess, and G. G. Gibson, 1990: Seasonal variation of cloud radiative forcing derived from the Earth Radiation Budget Experiment. *J. Geophys. Res.,* **94,** 18 687–18 703.

Harvey, L. D. D., 1988: On the role of high latitude ice, snow, and vegetation feedbacks in the climatic response to external forcing changes. *Clim. Change,* **13,** 191–224.

Hegg, D. A., P. V. Hobbs, and L. F. Radke, 1984: Measurements of the scavenging of sulfate and nitrate in clouds. *Atmos. Environ.,* **18,** 1939–1946.

Heitzenberg, J., H-C. Hansson, D. S. Covert, J-P. Blanchet, and J. A. Ogren, 1986: Physical and chemical properties of Arctic aerosols and clouds. *Arctic Air Pollution,* B. Stonehouse, Ed., Cambridge University Press, 25–35.

Henderson, P. M., 1967: Cloud conditions over the Beaufort Sea. Arctic Meteorology Research Group, Department of Meteorology, McGill University, Montreal, Pub. No. 86, 48 pp.

Herman, G. F., 1975: Radiative–diffusive models of the Arctic boundary layer, Department of Meteorology, Massachusetts Institute of Technology, Cambridge, 170 pp.

——, 1977: Solar radiation in the summer Arctic stratus clouds. *J. Atmos. Sci.,* **34,** 1425–1432.

——, 1980: Thermal radiation in Arctic stratus clouds. *Quart. J. Roy. Meteor. Soc.,* **106,** 771–780.

——, and R. Goody, 1976: Formation and persistence of summertime Arctic stratus clouds. *J. Atmos. Sci.,* **33,** 1537–1553.

——, and W. T. Johnson, 1980: Arctic and Antarctic climatology of a GLAS general circulation model. *Mon. Wea. Rev.,* **108,** 1974–1991.

——, and J. A. Curry, 1984: Observational and theoretical studies of solar radiation in Arctic stratus clouds. *J. Climate Appl. Meteor.,* **23,** 5–24.

Heymsfield, A. J., and C. M. R. Platt, 1984: A parameterization of the particle size spectrum of ice clouds in terms of the ambient temperature and the ice water content. *J. Atmos. Sci.,* **41,** 846–855.

Hobbs, P. V., G. C. Bluhm, and T. Ohtake, 1971: Transport of ice nuclei over the North Pacific Ocean. *Tellus,* **23,** 28–39.

Hoff, R. M., 1988: Vertical structure of Arctic haze observed by lidar. *J. Appl. Meteor.,* **27,** 125–139.

——, and W. R. Leaitch, 1989: Ground-based cirrus clouds in the Arctic. Preprints, *Symp. on the Role of Clouds in Atmospheric Chemistry and Global Climate,* Anaheim, CA, Amer. Meteor. Soc., 324–327.

Holmgren, B., L. Spears, C. Wilson, and C. S. Benson, 1975: Acoustic soundings of the Fairbanks temperature inversions. *Climate of the Arctic,* G. Weller and S. A. Bowling, Eds., Geophysical Institute, 293–306.

Houghton, J. T., G. J. Jenkins, and J. J. Ephraums, 1990: *Climate Change. The IPCC Scientific Assessment. World Meteorological*

Organization/United Nations Environment Programme. Cambridge University Press, 365 pp.
Hughes, N. A., 1984: Global cloud climatologies: An historical review. *J. Climate Appl. Meteor.,* **23,** 724–751.
Huschke, R. E., 1969: Arctic cloud statistics from "air-calibrated" surface weather observations. The Rand Corporation, RM-6173-PR, 79 pp.
Ingram, W. J., C. A. Wilson, and J. F. B. Mitchell, 1989: Modeling climate change: An assessment of sea ice and surface albedo feedbacks. *J. Geophys. Res.,* **94,** 8609–8622.
IPCC, 1990: Climate Change: *The IPCC Scientific Assessment.* J. T. Houghton, G. J. Jenkins, and J. J. Ephraums, Eds., Cambridge University Press, 365 pp.
Isono, K., M. Kombayasi, T. Takeda, T. Tanaka, K. Iwai, and M. Fijiwara, 1971: Concentration and nature of ice nuclei in rim of the North Pacific Ocean. *Tellus,* **23,** 40–59.
Jayaweera, K. O. L. F., and T. Ohtake, 1973: Concentration of ice crystals in Arctic stratus clouds. *J. Rech. Atmos.,* **7,** 199–207.
——, and P. Flanegan, 1982: Investigation of biogenic ice nuclei in the Arctic atmosphere. *Geophys. Res. Lett.,* **9,** 94–97.
Jin, Z., W. F. Weeks, S.-C. Tsay, and K. Stamnes, 1994: The effect of sea ice on the solar energy budget in the atmosphere-sea ice-ocean system: A model study. *J. Geophys. Res.,* **99**(C12), 25 281–25 294.
Johannessen, O. M., M. Miles, and E. Bjorgo, 1995: The Arctic's shrinking sea ice. *Nature,* **376,** 126–127.
Kahl, J. D., 1990: Characteristics of the low-level temperature inversion along the Alaskan Arctic coast. *Int. J. Climatol.,* **10,** 537–548.
——, M. C. Serreze, and R. C. Schnell, 1992: Low-level tropospheric temperature inversions in the Canadian Arctic. *Atmos.–Ocean,* **30,** 511–529.
——, D. J. Charlevoix, N. A. Zaitseva, R. C. Scnell, and M. C. Serreze, 1993: Absence of evidence for greenhouse warming over the Arctic Ocean during the past 40 years. *Nature,* **361,** 335–337.
Kellogg, W. W., 1973: Climatic feedback mechanisms involving the polar regions. *Climate of the Arctic,* G. Weller and S. A. Bowling, Eds., Geophysical Institute, Fairbanks, AK, 111–116.
Kent, G. S., L. R. Poole, and M. P. McCormick, 1986: Characteristics of arctic polar stratospheric clouds as measured by airborne lidar. *J. Atmos. Sci.,* **43,** 2149–2161.
Kergomard, C., B. Bonnela, and Y. Fouquart, 1993: Retrieval of surface radiative fluxes on the marginal zone of sea ice from operational satellite data. *Ann. Glaciol.,* **17,** 201–206.
Key, J., 1990: Cloud cover analysis with Arctic Advanced Very High Resolution Radiometer data. 2. Classification with spectral and textural measures. *J. Geophys. Res.,* **95,** 7661–7675.
——, and R. G. Barry, 1989: Cloud cover analysis with Arctic AVHRR data. 1. Cloud detection. *J. Geophys. Res.,* **94,** 8521–8535.
——, and M. Haefliger, 1992: Arctic ice surface temperature retrieval from AVHRR thermal channels. *J. Geophys. Res.,* **97**(D5), 5885–5893.
——, R. Stone, and M. Rehder, 1994: Estimating high latitude radiative fluxes from satellite data: Problems and successes. IGARSS 1018–1020.
Khattsov, V. M., T. V. Pavlova, and V. A. Govorkova, 1995: Heat and water budgets over the Northern Polar Region as estimated from 14 Atmospheric General Circulation Models. Voeikov Main Geophysical Observatory, St. Petersburg, Russia, unpublished manuscript, 30 pp.
Klinker, E., 1992: The verification of model radiation fluxes using satellite measurements. WCRP Rep. on a Workshop on Polar Radiation Fluxes and Sea-Ice Modelling. E. Raschke, H. Cattle, P. Lemke, and W. Rossow, Eds., WMO/TD, 62–66.
Koptev, A. P., and A. I. Voskresenskii, 1962: On the radiation properties of clouds. *Proc. Arctic and Antarctic Res. Inst.,* **239**(2), 39–47.
Kuhn, M., 1985: Bidirectional reflectance of polar and alpine snow surfaces. *Ann. Glaciol.,* **6,** 164–167.
Kukla, G., and D. Robinson, 1988: Variability of summer cloudiness in the Arctic Basin. *Meteor. Atmos. Phys.,* **39,** 42–50.
Langleben, M. P., 1969: Albedo and degree of puddling of a melting cover of sea ice. *J. Glaciol.,* **8,** 407–412.
——, 1971: Albedo of melting sea ice in the southern Beaufort Sea. *J. Glaciol.,* **10,** 101–104.
Lappen, C.-L., 1995: Comparison of the CSU GCM modeled climate with observations over the Arctic, Colorado State University Tech. Rep. in press.
Leaitch, R., R. M. Hoff, S. Melnichuk, and A. Hogan, 1984: Some physical and chemical properties of the arctic winter aerosol in northeastern Canada. *J. Climate Appl. Meteorol.,* **23,** 916–928.
Ledley, T. S., 1991: Snow on sea ice: Competing effects in shaping climate. *J. Geophys. Res.,* **96,** 17 195–17 208.
Leontyeva, E. N., and K. Stamnes, 1994: Estimations of cloud optical properties from ground-based measurements of incoming solar radiation in the Arctic. *J. Climate,* **7,** 566–578.
LeTreut, H., and Z.-X. Li, 1991: Sensitivity of an atmospheric general circulation model to prescribed SST changes: Feedback effects associated with the simulation of cloud optical properties. *Climate Dyn.,* **5,** 175–187.
Li, Z., and H. Leighton, 1991: Scene identification and its effect on cloud radiative forcing in the Arctic. *J. Geophys. Res.,* **96,** 9175–9188.
Lindsay, R. W., and D. A. Rothrock, 1994: Arctic sea ice surface temperature from AVHRR. *J. Climate,* **7,** 174–183.
Lynch, A. H., W. L. Chapman, J. E. Walsh, and G. Weller, 1995: Development of a regional climate model of the western Arctic. *J. Climate,* **8,** 1555–1570.
Manabe, S., and R. T. Wetherald, 1967: Thermal equilibrium of the atmosphere with a given distribution of relative humidity. *J. Atmos. Sci.,* **24,** 241–259.
——, R. J. Stoffer, M. J. Spelman, and K. Bryan, 1991: Transient response of a coupled ocean–atmosphere model to gradual changes of atmospheric CO_2. Part I: Annual mean response. *J. Climate,* **4,** 785–818.
Marshunova, M. S., 1961: Principle regularities of the radiation balance of the underlying surface and of the atmosphere in the Arctic (in Russian). *Tr. Arct. Antarct. Nauchno-Issled. Inst.,* **229**(5), Transl. by Rand Corp. Memo RM-5003-PR, 51-103.
——, and N. T. Chernigovsky, 1966: Numerical characteristics of the radiation regime in the Soviet Arctic. Proc. Symp. Arctic Heat Budget and Atmospheric Circulation. Rand Corp. Memo. RM-5233-NFS, 281-297.
——, and A. A. Mishin, 1995: Handbook of the Radiation Regime of the Arctic Basin (Results from the Drift Stations), Tech. Rep. APL-UW TR 9413, Applied Physics Laboratory, University of Washington.
Maxwell, J. B., 1982: The climate of the Canadian Arctic islands and adjacent waters. Vol. 2, *Climatological Studies,* Canadian Govt. Publishing Centre, Ministry of Supply and Services Canada, Ottawa, Canada, 30 pp.
Maykut, G. A., 1986: Surface heat and mass balance. *The Geophysics of Sea Ice,* N. Untersteiner, Ed., Plenum, 395–463.
——, and P. E. Church, 1973: Radiation climate of Barrow, Alaska 1962–1966. *J. Appl. Meteor.,* **12,** 620–628.
McCormick, M. P., and C. R. Trepte, 1987: Polar stratospheric optical depth observed between 1978 and 1985. *J. Geophys. Res.,* **92,** 4297–4306.
McCracken, M. C., R. D. Cess, and G. L. Potter, 1986: Climatic effects of anthropogenic arctic aerosols: An illustration of climatic feedback mechanisms with one- and two-dimensional climate models. *J. Geophys. Res.,* **91,** 14 455–14 450.
McGuffie, K., R. G. Barry, A. Schweiger, D. A. Robinson, and J. Newell, 1988: Intercomparison of satellite-derived cloud analyses for the Arctic Ocean in spring and summer. *Int. J. Remote Sens.,* **9,** 447–467.
McInnes, K. L., and J. A. Curry, 1995a: Modeling the mean and turbulent structure of the summertime Arctic cloudy boundary layer. *Bound.-Layer Meteor.,* **73,** 125–143.

——, and ——, 1995b: Life cycles of summertime Arctic stratus clouds. Preprints, *Fourth Conf. on Polar Meteorology and Oceanography.* Dallas, TX, Amer. Meteor. Soc., (J12)1–(J12)3.

Minnis, P., P. W. Heck, and D. F. Young, 1993: Inference of cirrus cloud properties using satellite-observed visible and infrared radiances. Part II: Verification of theoretical cirrus radiative properties. *J. Atmos. Sci.,* **50,** 1305–1322.

Mitchell, J. F. B., and W. J. Ingram, 1992: Carbon dioxide and climate: Mechanisms of changes in cloud. *J. Climate,* **5,** 5–21.

——, C. A. Senior, and W. J. Ingram, 1989: CO_2 and climate: A missing feedback? *Nature,* **341,** 132–134.

Mokhov, I. I., and M. E. Schlesinger, 1993: Analysis of global cloudiness. 1: Comparison of ISCCP, Meteor and Nimbus 7 satellite data. *J. Geophys. Res.,* **98,** 12 849–12 868.

——, and ——, 1994: Analysis of global cloudiness. 2: Comparison of ground-based and satellite-based climatologies. *J. Geophys. Res.,* **99,** 17 045–17 065.

Moritz, R. E., J. A. Curry, A. S. Thorndike, and N. Untersteiner, 1993: Surface heat budget of the Arctic Ocean. Rep. 3, ARCSS OAII Science Management Office, Polar Science Center, APL-UW, 34 pp. [University of Washington, Seattle, WA, 98105.]

Nakamura, N., and A. H. Oort, 1988: Atmospheric heat budget of the polar regions. *J. Geophys. Res.,* **93,** 9510–9524.

Nansen, F., 1897: In Nacht und Eis. *Die Norwegische Polar-Expedition, 1893–1896,* Vol. 1, Brokhaus.

Nemesure, S., R. D. Cess, and E. G. Dutton, 1994: Impact of clouds on the shortwave radiation budget of the surface-atmosphere system for snow-covered surfaces. *J. Climate,* **7,** 579–585.

Ohmura, A., and H. Gilgen, 1991: Global Energy Balance Archive GEBA. Report 2: The GEBA database, interactive applications, retrieving data. Internal Report, 66 pp. [Available from Department of Geography, ETH-Zurich, Winterthurerstrasse 190, CH-8057 Zurich, Switzerland.]

Ohtake, T., 1993: Freezing points of H_2SO_4 aqueous solutions and formation of stratospheric ice clouds. *Tellus,* **45**(B), 138–144.

——, K. O. L. F. Jayaweera, K.-I. Sakurai, 1982: Observation of ice crystal formation in lower Arctic atmosphere. *J. Atmos. Sci.,* **39,** 2898–2904.

Overland, J. E., and P. S. Guest, 1991: The Arctic snow and air temperature budget over sea ice during winter. *J. Geophys. Res.,* **96,** 4651–4662.

Patterson, E. M., B. T. Marshall, and K. A. Rahn, 1982: Radiative properties of the arctic aerosol. *Atmos. Environ.,* **16,** 2967–2977.

Perovich, D. K., 1991: Seasonal changes in sea ice optical properties during fall freeze-up. *Cold Reg. Sci. Technol.,* **19,** 261–273.

——, 1994: Light reflection from sea ice during the onset of melt. *J. Geophys. Res.,* **99**(C2), 3351–3359.

——, and T. C. Grenfell, 1981: Laboratory studies of the optical properties of young sea ice. *J. Glaciol.,* **27,** 331–346.

——, G. A. Maykut, and T. C. Grenfell, 1986: Optical properties of ice and snow in the polar oceans. I: Observations, Ocean Optics 8. *Proc. SPIE Int. Soc. Opt. Eng.,* **637,** 232–241.

Pinto, J. O., and J. A. Curry, 1995: Atmospheric convective plumes emanating from leads. 2: Microphysical and radiative processes. *J. Geophys. Res.,* **100,** 4633–4642.

——, and ——, 1996: Role of radiative transfer in the modeled mesoscale development of summertime arctic stratus. *J. Geophys. Res.,* in press.

——, ——, and K. L. McInnes, 1995a: Atmospheric convective plumes emanating from leads. 1: Thermodynamic structure. *J. Geophys. Res.,* **100,** 4621–4631.

——, ——, and C. W. Fairall, 1995b: Radiative and microphysical properties of low-level Arctic clouds inferred from ground-based measurements. *J. Geophys. Res.,* in press.

Platt, C. M. R., and Harshvardhan, 1988: Temperature dependence of cirrus extinction: Implications for climate feedback. *J. Geophys. Res.,* **93,** 11 051–11 058.

Putnins, P., 1970: The climate of Greenland. *Climates of Polar Regions,* Vol. 14, *World Survey of Climatology,* S. Orvig, Ed., Elsevier, 3–128.

Radke, L. F., and P. V. Hobbs, 1969: Measurement of cloud condensation nuclei, light scattering coefficient, sodium containing particles, and Aitken Nuclei in the Olympic Mountains of Washington. *J. Atmos. Sci.,* **26,** 281–288.

——, ——, and J. E. Pinnons, 1976: Observations of cloud condensation nuclei, sodium-containing particles, ice nuclei and the light-scattering coefficient near Barrow, Alaska. *J. Appl. Meteor.,* **15,** 982–995.

Rahn, K. A., R. D. Borys, and G. E. Shaw, 1977: Asian source of Arctic haze bands. *Nature,* **268,** 713–715.

Ramanathan, V., R. D. Cess, E. F. Harrison, P. Minnis, B. R. Barkstrom, E. Ahmad, and D. Hartman, 1989: Cloud-radiative forcing and climate: Results from the Earth Radiation Budget Experiment. *Science,* **243,** 57–63.

Randall, D. A., J. A. Abeles, and T. G. Corsetti, 1985: Seasonal simulations of the planetary boundary layer and boundary layer stratocumulus clouds with a general circulation model. *J. Atmos. Sci.,* **42,** 641–676.

Raschke, E., 1987: Report of the International Satellite Cloud Climatology Project (ISCCP). Workshop on Cloud Algorithms on the Polar Regions, WCP-131, WMO/TD-No. 170, WMO, Geneva.

——, P. Bauer, and H. J. Lutz, 1992: Remote sensing of clouds and surface radiation budget over polar regions. *Int. J. Remote Sensing,* **13,** 13–22.

Rathore, R. S., 1983: Cloud microphysical studies in the Arctic. M.S. thesis, Department of Marine Earth and Atmospheric Sciences, North Carolina State University, 68 pp.

Robinson, D. A., M. C. Serreze, R. G. Barry, G. Scharfen, and G. Kukla, 1992: Large-scale patterns and variability of snowmelt and parameterized surface albedo in the Arctic Basin. *J. Climate,* **5,** 1109–1119.

Robock, A., 1983: Ice and snow feedbacks and the latitudinal and seasonal distribution of climate sensitivity. *J. Atmos. Sci.,* **40,** 986–997.

Rosen, H., T. Novakov, and B. A. Bodhaine, 1981: Soot in the Arctic. *Atmos. Environ.,* **15,** 1371–1374.

Rossow, W. B., 1995: Another look at the seasonal variation of polar cloudiness with satellite and surface observations. Preprints, *Fourth Conf. on Polar Meteorology and Oceanography,* Dallas, TX, Amer. Meteor. Soc., (J10)1–(J10)4.

——, and R. A. Schiffer, 1991: ISCCP cloud data products. *Bull. Amer. Meteor. Soc.,* **72,** 2–20.

——, and L. C. Garder, 1993: Validation of ISCCP cloud detections. *J. Climate,* **6,** 2370–2393.

——, and Y.-C. Zhang, 1995: Calculation of surface and top-of-atmosphere radiative fluxes from physical quantities based on ISCCP datasets. Part II: Validation and first results. *J. Geophys. Res.,* **100,** 1167–1197.

——, A. W. Walker, and L. C. Garder, 1993: Comparison of ISCCP and other cloud amounts. *J. Climate,* **6,** 2394–2418.

Royer, J. F., S. Planto, and M. Deque, 1990: A sensitivity experiment for the removal of Arctic sea ice with the French spectral general circulation model. *Climate Dyn.,* **5,** 1–17.

Ruffieux, D., P. O. G. Persson, C. W. Fairall, and D. E. Wolfe, 1995: Ice pack and lead surface energy budgets during LEADEX 92. *J. Geophys. Res.,* **100,** 4593–4612.

Schlesinger, M. E., 1985: Analysis of results from energy balance and radiative-convective models. *Projecting the Climatic Effects of Increasing Carbon Dioxide,* M. C. MacCracken and F. M. Luther, Eds., U.S. Dept. Energy, DOE/ER-0237, 81–147.

——, and X. Jiang, 1991: Revised projection of future greenhouse warming. *Nature,* **350,** 219–221.

Schlosser, E., 1988: Optical studies of Antarctic sea ice. *Cold Reg. Sci. Technol.,* **15,** 289–293.

Schnell, R. C., R. G. Barry, M. W. Miles, E. L. Andreas, L. F. Radke, C. A. Brock, M. P. McCormick, and J. L. Moore, 1989: Lidar detection of leads in Arctic sea ice. *Nature,* **339,** 530–532.

Schweiger, J. A., and J. R. Key, 1992: Arctic cloudiness: Comparison of ISCCP-C2 and Nimbus-7 satellite-derived cloud products

with a surface-based cloud climatology. *J. Climate,* **5,** 1514–1527.
——, and ——, 1993: Arctic radiative fluxes and cloud forcing estimated from the ISCCP C2 cloud data set. Preprints, *Third Conf. on Polar Meteorology and Oceanography,* Portland, OR, Amer. Meteor. Soc., 13–16.
——, and ——, 1994: Arctic Ocean radiative fluxes and cloud forcing estimated from the ISCCP C2 cloud dataset, 1983–1990. *J. Appl. Meteor.,* **33,** 948–963.
——, M. C. Serreze, and J. R. Key, 1993: Arctic sea ice albedo: A comparison of two satellite-derived data sets. *Geophys. Res. Lett.,* **20,** 41–44.
Sedunov, Y. S., 1974: *Physics of Drop Formation in the Atmosphere.* Keter.
Sellers, W. D., 1969: A global climate model based on the energy balance of the earth–atmosphere system. *J. Appl. Meteor.,* **8,** 392–400.
Serreze, M. C., J. D. Kahl, and R. C. Schnell, 1992: Low-level temperature inversions of the Eurasian Arctic and comparisons with Soviet ice island data. *J. Climate,* **5,** 599–613.
——, R. G. Barry, and J. E. Walsh, 1995a: Atmospheric water vapor characteristics at 70°N. *J. Climate,* **8,** 719–731.
——, M. C. Rehder, R. G. Barry, J. D. Kahl, and N. A. Zaitseva, 1995b: The distribution and transport of atmospheric water vapor over the Arctic basin. *Int. J. Clim.,* **15,** 709–727.
Shaw, G. E., 1983: Bio-controlled thermostasis involving the sulfur cycle. *Climate Change,* **5,** 297–303.
——, 1986: Aerosols in Alaskan air masses. *J. Atmos. Chem.,* **4,** 157–171.
——, 1987: Aerosols as climate regulators: A climate biosphere linkage? *Atmos. Environ.,* **21,** 985–986.
——, and G. Wendler, 1972: Atmospheric turbidity measurements at McCall Glacier in northeast Alaska. *Conf. on Atmospheric Radiation,* Ft. Collins, CO, Amer. Meteor. Soc., 181–187.
——, and K. Stamnes, 1980: Arctic haze: A perturbation of the polar radiation budget. *Ann. N. Y. Acad. Sci.,* **338,** 533–539.
Shine, K. P., 1984: Parameterization of shortwave flux over high albedo surfaces as a function of cloud thickness and surface albedo. *Quart. J. Roy. Meteor. Soc.,* **110,** 747–764.
——, and A. Henderson-Sellers, 1985: The sensitivity of a thermodynamic sea ice model to changes in surface albedo parameterization. *J. Geophys. Res.,* **90,** 2243–2250.
Skony, S. M., N. A. Zaitseva, and J. D. W. Kahl, 1994: Differences between radiosonde and dropsonde temperature profiles over the Arctic Ocean. *J. Atmos. Oceanic Technol.,* **11,** 1400.
Somerville, R. C., and L. A. Remer, 1984: Cloud optical thickness feedbacks in the CO_2 climate problem. *J. Geophys. Res.,* **89,** 9668–9672.
Spelman, M. J., and S. Manabe, 1984: Influence of oceanic heat transport upon the sensitivity of a model climate. *J. Geophys. Res.,* **89,** 571–586.
Steffen, K., 1987: Bidirectional reflectance of snow at 500–600 nm. *Large Scale Effects of Seasonal Snowcover.* IAHS Publ., 166, 415–425.
——, and T. DeMaria, 1995: Surface energy balance of arctic sea ice in winter. Preprints, *Fourth Conf. on Polar Meteorology and Oceanography.* Dallas, TX, Amer. Meteor. Soc., 75–78.
Stephens, G. L., 1978: Radiation profiles in extended water clouds. *J. Atmos. Sci.,* **35,** 2111–2222.
——, 1990: On the relationship between water vapor over the oceans and sea surface temperature. *J. Climate,* **3,** 634–645.
——, and T. J. Greenwald, 1991: The earth's radiation budget and its relation to atmospheric hydrology. 2: Observations of cloud effects. *J. Geophys. Res.,* **96,** 15 325–15 340.
Stonehouse, B., 1986: *Arctic Air Pollution.* Cambridge University Press, 328 pp.
Sverdrup, H. U., 1933: *The Norwegian North Polar Expedition with the "Maud", 1918–1925, Scientific Results.* Vol. 1a. Geofysik Institutt, 331 pp.
Tao, X., W. L. Chapman, and J. E. Walsh, 1995: Intercomparison of global climate model simulations of Arctic temperature. Preprints, *Fourth Conf. on Polar Meteorology and Oceanography,* Dallas, TX, Amer. Meteor. Soc., 138–143.
Taylor, K. E., and S. J. Ghan, 1992: An analysis of cloud liquid water feedback and global climate sensitivity in a general circulation model. *J. Climate,* **5,** 907–919.
Telford, J. W., and S. K. Chai, 1980: A new aspect of condensation theory. *Pure Appl. Geophys.,* **118,** 720–742.
——, and P. B. Wagner, 1981: Observations of condensation growth determined by entity type mixing. *Pure Appl. Geophys.,* **119,** 934–965.
Thorndike, A. S., R. Colony, and E. Munoz, 1983: Arctic Ocean Buoy Program Data Report, Polar Science Center, University of Washington, Seattle, 132 pp.
Thuman, W. C., and E. Robinson, 1954: Studies of Alaskan ice fog particles. *J. Meteor.,* **11,** 151–156.
Trivett, N., L. Barrie, and J. Bottenhein, 1988: An experimental investigation of arctic haze at Alert, N.W.T., March 1985. *Atmos.-Ocean,* **26,** 341–376.
Tsay, S.-C., and K. Jayaweera, 1984: Physical characteristics of arctic stratus clouds. *J. Climate Appl. Meteor.,* **23,** 584–596.
——, K. Stamnes, and K. Jayaweera, 1989: Radiative energy budget in the cloudy and hazy Arctic. *J. Atmos. Sci.,* **46,** 1102–1018.
Tselioudis, G., and W. B. Rossow, 1994: Global, multiyear variations of optical thickness with temperature in low and cirrus clouds. *Geophys. Res. Lett.,* **21,** 2211–2214.
——, D. Rind, and W. B. Rossow, 1992: Global patterns of cloud optical thickness variation with temperature. *J. Climate,* **5,** 1484–1495.
——, A. A. Lacis, and D. Rind, 1993: Potential effects of cloud optical thickness on climate warming. *Nature,* **366,** 670–672.
Twomey, S., 1977: *Atmospheric Aerosols.* Elsevier, 287–290.
——, 1991: Aerosols, clouds and radiation. *Atmos. Environ.,* **25A,** 2435–2442.
Tzeng, R.-Y., and D. H. Bromwich, 1994: NCAR CCM2 simulation of present-day arctic climate. Preprints, *Sixth Conf. on Climate Variations.* Nashville, TN, Amer. Meteor. Soc., 197–201.
Valero, F. P. J., and T. P. Ackerman, 1986: Arctic haze and the radiation balance. *Arctic Air Pollution,* B. Stonehouse, Ed., Cambridge University Press, 121–133.
Vedder, J. F., E. P. Condon, E. C. Y. Inn, K. D. Tabor, and M. A. Kritz, 1987: Measurements of stratospheric SO2 after the El Chichon eruptions. *Geophys. Res. Lett.,* **10,** 1045–1048.
Vowinckel, E., 1962: Cloud amount and type over the Arctic. *Publication in Meteorology,* No. 51, pp. 27.
——, and S. Orvig, 1964: Radiation balance of the troposphere and of the earth-atmosphere system in the Arctic. McGill University (AFCRL 64-35), 370 pp.
——, and ——, 1970: The climate of the North Polar Basin. *Climates of the Polar Regions, Vol. 14, World Survey of Climatology,* S. Orvig, Ed., Elsevier, 129–152.
Walsh, J. E., 1983: The role of sea ice in climatic variability: Theories and evidence. *Atmos.-Ocean,* **21,** 229–242.
——, and R. G. Crane, 1992: A comparison of GCM simulations of arctic climate. *Geophys. Res. Lett.,* **19,** 29–32.
——, A. Lynch, and W. Chapman, 1993: A regional model for studies of atmosphere–ice–ocean interaction in the western Arctic. *Meteor. Atmos. Phys.,* **51,** 179.
Warren, S. G., and W. J. Wiscombe, 1980: A model for the spectral albedos of snow. Part II: Effects of aerosols. *J. Atmos. Sci.,* **37,** 2734–2750.
——, D. Hahn, and J. London, 1980: Ground-based observations of cloudiness for cross-validation of satellite observations. *Workshop Rep. on Clouds in Climate: Modeling and Satellite Observational Studies,* New York, NY, NASA Goddard Institute for Space Studies, 174–179.
——, C. J. Hahn, J. London, R. M. Chervin, and R. L. Jenne, 1988: Global Distribution of Total Cloud Cover and Cloud Type Amounts over the Ocean. NCAR/TN-317+STR, 212 pp.
Warshaw, M., and R. P. Rapp, 1973: An experiment on the sensitivity of a global circulation model. *J. Appl. Meteor.,* **12,** 43–49.

Washington, W. W., and G. A. Meehl, 1986: General circulation model CO_2 sensitivity experiments: Snow-sea ice albedo parameterizations and globally averaged surface air temperature. *Clim. Change,* **8,** 231–241.

WCRP, 1992: *Report on a Workshop on Polar Radiation Fluxes and Sea-Ice Modelling.* E. Raschke, H. Cattle, P. Lemke, and W. Rossow, Eds., WMO/TD, 112 pp.

Webb, M. J., A. Slingo, and G. L. Stephens, 1993: Seasonal variations of the clear-sky greenhouse effect: The role of changes in atmospheric temperatures and humidities. *Climate Dyn.,* **9,** 117–129.

Welch, R. M., S. K. Cox, and J. M. Davis, 1980: *Solar Radiation and Clouds. Meteor. Monogr.,* No. 39, Amer. Meteor. Soc., 96 pp.

——, S. K. Sengupta, A. K. Goroch, P. Rabindra, N. Rangaraj, and M. S. Navar, 1992: Polar cloud and surface classification using AVHRR imagery: An intercomparison of methods. *J. Appl. Meteor.,* **31,** 405–420.

Wendler, G., 1972: Effect of arctic stratus clouds on the radiation regime. *Studies of the Solar and Terrestrial Radiation Fluxes over Arctic Pack Ice.* ARPA, 33 pp.

——, and F. Eaton, 1990: Surface radiation budget at Barrow, Alaska. *Theor. Appl. Climatol.,* **41,** 107–115.

Wetherald, R. T., and S. Manabe, 1980: Cloud cover and climate sensitivity. *J. Atmos. Sci.,* **37,** 1485–1510.

——, and ——, 1986: An investigation of cloud cover change in response to thermal forcing. *Clim. Change,* **8,** 5–24.

——, and ——, 1988: Cloud feedback processes in a general circulation model. *J. Atmos. Sci.,* **45,** 1397–1415.

Wexler, H., 1936: Cooling in the lower atmosphere and the structure of polar continental air. *Mon. Wea. Rev.,* **64,** 122–136.

Williamson, D. L., and P. J. Rasch, 1994: Water vapor transport in the NCAR CCM2. *Tellus,* **46,** 34–51.

Wilson, C. A., and J. F. B. Mitchell, 1987: A $2 \times CO_2$ climate sensitivity experiment with a global climate model including a simple ocean. *J. Geophys. Res.,* **92,** 13 315–13 343.

Wilson, L. D., J. A. Curry, and T. P. Ackerman, 1993: On the satellite retrieval of lower tropospheric ice crystal clouds in the polar regions. *J. Climate,* **6,** 1467–1472.

Wiscombe, W., 1975: Solar radiation calculations for arctic summer stratus conditions. *Climate of the Arctic,* G. Weller, and S. A. Bowling, Eds., Geophysical Institute, 245–254.

——, and S. G. Warren, 1980: A model for the spectral albedos of snow. Part I: Pure snow. *J. Atmos. Sci.,* **37,** 2712–2733.

Witte, H. J., 1968: Airborne observations of cloud particles and infrared flux density in the Arctic. MS Thesis, Dept. of Atmospheric Sciences, University of Washington. 102 pp.

Yamanouchi, T., and S. Kawaguchi, 1992: Cloud distribution in the Antarctic from AVHRR data and radiation measurements at the surface. *Int. J. Remote Sens.,* **13,** 111–127.

Zavarina, M. V., and M. K. Romasheva, 1957: Thickness of clouds over Arctic seas and over the central Arctic. *Probl. Arkt.,* **2.**

Zhang, M. H., J. J. Hack, J. T. Kiehl, and R. D. Cess, 1994: Diagnostic study of climate feedback processes in atmospheric general circulation models. *J. Geophys. Res.,* **99**(D3), 5525–5537.

Zhang, Y.-C., W. B. Rossow, and A. A. Lacis, 1995: Calculation of surface and top-of-atmosphere radiative fluxes from physical quantities based on ISCCP datasets. Part I: Method and sensitivity to input data uncertainties. *J. Geophys. Res.,* **100,** 1149–1165.